IEEE Access
Multidisciplinary ⋮ Rapid Review ⋮ Open Access Journal

Received September 17, 2021, accepted October 7, 2021, date of publication October 13, 2021, date of current version October 22, 2021.

Digital Object Identifier 10.1109/ACCESS.2021.3119570

P-Rob Six-Degree-of-Freedom Robot Manipulator Dynamics Modeling and Anti-Disturbance Control

CHANG ZHANG AND YUQIANG WU
School of Engineering, Qufu Normal University, Rizhao 276826, China
Corresponding author: Yuqiang Wu (yu_qiang_wu@126.com)

This work was supported in part by the National Natural Science Foundation of China under Grant 62073187, and in part by the Major Research Project of Shandong Province under Grant 2019JZZY011111.

ABSTRACT In this paper, the problem of modeling and anti-disturbance control is studied for lightweight personal robotics (P-Robs) with a six-degree-of-freedom robot manipulator to solve the movement instability phenomenon caused by time-varying uncertain disturbances during the movement of the robot manipulator. The detailed dynamical equations of the P-Rob system are solved based on the Lagrange energy equation, and the actual dynamical model of the robot manipulator system is obtained. The disturbance observer is designed to estimate the disturbance effectively, and an integral sliding mode control algorithm is proposed to realize tracking control. Stability analysis of the system is carried out using the Lyapunov function. Finally, experiments are conducted on an actual P-Rob system model, and the experimental results show that the robot manipulator system tracks the desired trajectory effectively, which validates the effectiveness of the proposed control algorithm.

INDEX TERMS P-Rob system, robot manipulator, dynamical modeling, disturbance observer, integral sliding mode control, trajectory tracking.

I. INTRODUCTION

In recent years, service-type six-degree-of-freedom robots have been widely used. In the field of intelligent medicine, quadriplegic patients can reach and grasp imaginary objects through a neural-controlled robot manipulator [1]. In laboratory automation production, an ideal six-degree-of-freedom robot manipulator automatic synthesis platform is used to complete the unmanned compound automatic production process [2]. In the packaging industry, the use of mobile six-degree-of-freedom robot manipulators and the design of automatic wrappers have enabled the fast and accurate packaging of objects [3]. In a complex working environment, the robot manipulator can collaborate with humans to complete the task and improve work efficiency [4].

Sliding mode control [5]–[11], which has the advantage of not relying on the precise structure of the system, has been widely used in the control of robots and has achieved more results. In [12], for a sensor-less telerobotic system, it is proposed a variable structure control with neural network and optimized fractional-order selection policy. In [13], to improve the tracking performance of wafer stages for semiconductor manufacturing. Based on sliding mode control (SMC), a practical fractional-order variable gain super-twisting algorithm (PFVSTA) is proposed. In [14], sliding mode controllers are designed for regulating the dead zone and gravity unknown behavior of the robot manipulator. In [15], effective control of a service robot manipulator is achieved using an improved sliding mode index arrival rate. Reference [16] presented a radical adaptive terminal sliding mode control method for robot manipulators with model uncertainties and external disturbances.

Robot manipulator systems are often subject to various uncertain external perturbations and modeling inaccuracy problems in practical applications, so anti-disturbance control and adaptive neural-network control has successfully been used to solve the control problems of robot manipulators. A control scheme based on a disturbance observer is proposed for robot manipulators with internal and external disturbances in [17]. In [18], a general framework is proposed for disturbed nonlinear systems using disturbance observer-based control (DOBC) techniques. It is also applied to a two-linked robot manipulator. To solve the trajectory tracking problem of the underwater manipulator for the set-total perturbation, a fractional integral sliding mode control strategy with a perturbation observer is proposed [19]. Combined with the design of the disturbance observer, in the general case, the literature [20]–[22] considered the external

The associate editor coordinating the review of this manuscript and approving it for publication was Mohammad Alshabi.

disturbance as an unknown bounded constant, which in turn gave the anti-disturbance control of the robot manipulator. References [23] proposes an adaptive neural-network control scheme, an effective estimation of the unmodeled dynamics of the robotic manipulator system is performed. For the parameter uncertainty and model nonlinearity of the robotic arm system, an improved neural network control algorithm is proposed in the literature [24] to overcome the perturbation phenomenon of the system.

Based on the above literature, good research results are obtained for the sliding mode control of the robot manipulator system and various anti-disturbance controls. However, none of the above-mentioned literature has explored the applicability of the designed control algorithm on a real six-degree-of-freedom mathematical model. For the simulation tests, a two-degree-of-freedom or three-degree-of-freedom robotic arm model with a simpler mathematical model is chosen. The same problem occurs in the literature [25]–[32]. The kinematics of lightweight robot manipulators have been studied in the literature [33]–[35]. Through extensive literature reading, it is found that the lightweight robot manipulator is mainly oriented to real-life human-robot interaction applications with small motion speed for safety reasons. Therefore, there are more studies on the kinematics of lightweight robot manipulators and fewer studies on the dynamics. However, in the custom-oriented miniaturized rapid packaging line, an intelligent emerging manufacturing scenario, the dynamics of lightweight robotic arms are essential to study. Moreover, the modeling of six-degree-of-freedom robot manipulator systems is given only a general theoretical description in much of the literature, with no or very little literature providing a complete representation of the exact dynamics model. This leads to the fact that in practice when the studied control algorithm is applied to a six-degree-of-freedom robot manipulator system, it does not achieve a better control effect similar to that in the simulation.

This paper studies the dynamic modeling and anti-disturbance control of a lightweight six-degree-of-freedom robot manipulator. The rate of change of the total system disturbance is considered to be nonzero, and the global asymptotically stable convergence of the disturbance estimation error to zero is ensured by the reasonable design of the observer gain. The main work is reflected in the following aspects. Since the dynamics of lightweight robot manipulators are less studied, we investigated the dynamics of lightweight robot manipulators. The lightweight robot manipulator is sensitive to the dynamical parameters, which in turn poses certain challenges for dynamics modeling. For this reason, we have made reasonable assumptions in combination with the mechanical structure of the system and a form that more closely resembles real motion. To address the problem that much of the literature does not consider the actual mathematical model of the six-degree-of-freedom robot manipulator in its theoretical and simulation analysis, an accurate modeling calculation of the P-Rob six-degree-of-freedom robot manipulator system is carried out, and the specific dynamics model expression of the P-Rob system is solved based on the Lagrange equation. Design the disturbance observer and consider a non-zero rate of change of the total system disturbance. An integral sliding mode control algorithm based on a disturbance observer is proposed to achieve effective tracking of the desired trajectory of the system. Finally, the designed control algorithm is experimentally verified on an actual P-Rob robot manipulator platform based on the Python language.

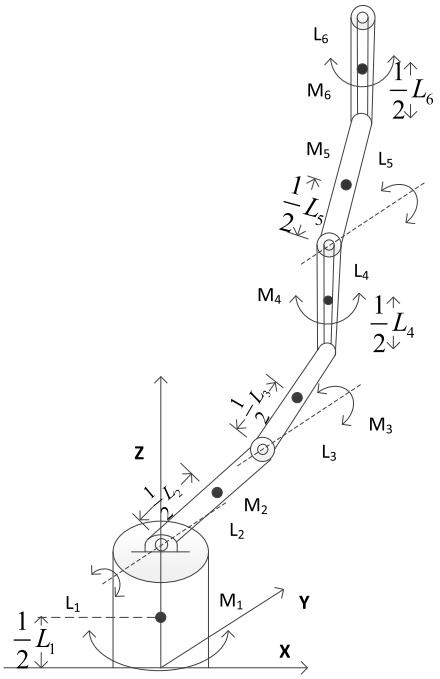

FIGURE 1. Robot manipulator model diagram.

II. P-ROB SYSTEM DYNAMICS MODEL CONSTRUCTION

To solve the complexity of the analysis of the actual model of the robot manipulator, it is convenient to solve and analyze the dynamic equations of the robot manipulator and then accurately obtain a system dynamics model. The model diagram is shown in Figure 1. There are many kinds of dynamic analysis methods for manipulator systems. The Lagrange equation is used in this system to derive the dynamics equation of P-Rob. The fundamental principle of the Lagrange method is the differentiation of each state in the system and time by combining the energy equation of the system, which only needs to analyze the kinetic energy and potential energy of the system without considering other problems [36].

To obtain the dynamics equations of the system, the kinetic energy and potential energy of the system should be solved, and then the Lagrange function should be established. Then, the partial derivatives of the system variables and time can be obtained by using the Lagrange function.

$$\begin{cases} L = K - P \\ \tau_i = \dfrac{\partial}{\partial t}\left(\dfrac{\partial L}{\partial \dot{\theta}_i}\right) - \dfrac{\partial L}{\partial \theta_i} \end{cases} \tag{1}$$

where L is the Lagrange function, K and P are the system kinetic energy and potential energy respectively; τ_i is the sum of the external torque that produces rotation; and θ_i is the system variable.

A. SOLVING FOR KINETIC ENERGY OF SYSTEM

The kinetic energy of each link is solved separately for the P-Rob six-degree-of-freedom manipulator, and the total kinetic energy of the system is finally obtained. We establish a right-angle coordinate system from the bottom of the base, denoted as $x_0y_0z_0$. Taking the center of each link as the center of mass position, according to the established Cartesian coordinate system, we can obtain the coordinates of the center of mass of each link. By deriving the coordinates of the center of mass of each linkage, the velocity component of the linkage on the three axes of the coordinate system is obtained and denoted as $\dot{x}_i, \dot{y}_i, \dot{z}_i$, $i = 1, 2, \ldots 6$. From formula $v_i = \sqrt{\dot{x}_i^2 + \dot{y}_i^2 + \dot{z}_i^2}$ can be obtained from the speed of the i th link, and then we get the i th link of the flat kinetic energy, plus the i th link of the kinetic energy of rotation. Then, we determine the total kinetic energy of the i th link through formula (2).

$$K_i = \frac{1}{2}\left(m_i v_i^2 + I_i \dot{\theta}_i^2\right) \tag{2}$$

where m_i is the mass of the i th joint, $\dot{\theta}_i$ is the angular velocity of each joint, and I_i is the rotational inertia of the ith linkage.

The six links are now analyzed separately for translational and rotational kinetic energies.

Assumption 1: Link 4 and link 6 are always parallel to link 1 during the movement and rotate around the same direction.

Remark 1: To facilitate the construction of the system dynamics model, it is assumed that link 4 and link 6 are always parallel to link 1 in the process of moving and only rotate in the vertical direction. This assumption is very reasonable. Combined with the mechanical structure of the system and through reasonable trajectory planning calculation, the motion of joint 2 and joint 3 can make link 4 parallel to link 1, and the motion of joint 2, joint 3, and joint 5 can make link 4 and link 6 parallel to link 1. Therefore, it can make the system achieve the grasping of the target object under the motion condition that link 4 and link 6 are always parallel to link 1.

Link 1: Only its rotational kinetic energy exists, so the kinetic energy of link 1 is

$$E_{k1} = \frac{1}{2} I_1 \dot{\theta}_1^2 \tag{3}$$

Link 2: There is translational kinetic energy and rotational kinetic energy, so the kinetic energy of link 2 is

$$E_{k2} = \frac{1}{2} m_2 v_2^2 + \frac{1}{2} I_2 \dot{\theta}_2^2 \tag{4}$$

Link 3: There is translational kinetic energy, rotational kinetic energy, and the influence of link 2 on the rotational kinetic energy of link 3, so the kinetic energy of link 3 is

$$E_{k3} = \frac{1}{2} m_3 v_3^2 + \frac{1}{2} I_3 \left(\dot{\theta}_2 + \dot{\theta}_3\right)^2 \tag{5}$$

Link 4: There is translational kinetic energy, rotational kinetic energy, and the influence of link 1 on the rotational kinetic energy of link 4. Thus, the kinetic energy of link 4 is

$$E_{k4} = \frac{1}{2} m_4 v_4^2 + \frac{1}{2} I_4 \left(\dot{\theta}_1 + \dot{\theta}_4\right)^2 \tag{6}$$

Link 5: There is translational kinetic energy, rotational kinetic energy, and the influence of links 2 and 3 on the rotational kinetic energy of link 5, so the kinetic energy of link 5 is

$$E_{k5} = \frac{1}{2} m_5 v_5^2 + \frac{1}{2} I_5 \left(\dot{\theta}_2 + \dot{\theta}_3 + \dot{\theta}_5\right)^2 \tag{7}$$

Link 6: There is translational kinetic energy, rotational kinetic energy, and the influence of links 1 and 4 on the rotational kinetic energy of link 6, so the kinetic energy of link 6 is

$$E_{k6} = \frac{1}{2} m_6 v_6^2 + \frac{1}{2} I_6 \left(\dot{\theta}_1 + \dot{\theta}_4 + \dot{\theta}_6\right)^2 \tag{8}$$

Now, we solve for the coordinates of the centroid of each link.

Link 1:

$$\begin{cases} x_1 = 0 \\ y_1 = 0 \\ z_1 = \dfrac{l_1}{2} \end{cases} \tag{9}$$

Link 2:

$$\begin{cases} x_2 = \dfrac{l_2}{2} c_2 c_1 \\ y_2 = \dfrac{l_2}{2} c_2 s_1 \\ z_2 = \dfrac{l_2}{2} s_2 + l_1 \end{cases} \tag{10}$$

Link 3:

$$\begin{cases} x_3 = \left(l_2 c_2 + \dfrac{l_3}{2} c_{23}\right) c_1 \\ y_3 = \left(l_2 c_2 + \dfrac{l_3}{2} c_{23}\right) s_1 \\ z_3 = \dfrac{l_3}{2} s_{23} + l_2 s_2 + l_1 \end{cases} \tag{11}$$

Link 4:

$$\begin{cases} x_4 = \left(l_2 c_2 + \dfrac{l_3}{2} c_{23}\right) c_1 \\ y_4 = \left(l_2 c_2 + \dfrac{l_3}{2} c_{23}\right) s_1 \\ z_4 = \dfrac{l_4}{2} + l_3 s_{23} + l_2 s_2 + l_1 \end{cases} \tag{12}$$

Link 5:

$$\begin{cases} x_5 = \left(l_2c_2 + l_3c_{23} + \dfrac{l_5}{2}c_{235}\right)c_1 \\ y_5 = \left(l_2c_2 + l_3c_{23} + \dfrac{l_5}{2}c_{235}\right)s_1 \\ z_5 = \dfrac{l_5}{2}s_5 + l_4 + l_3s_{23} + l_2s_2 + l_1 \end{cases} \tag{13}$$

Link 6:

$$\begin{cases} x_6 = \left(l_2c_2 + l_3c_{23} + \dfrac{l_5}{2}c_{235}\right)c_1 \\ y_6 = \left(l_2c_2 + l_3c_{23} + \dfrac{l_5}{2}c_{235}\right)s_1 \\ z_6 = \dfrac{l_6}{2} + l_5s_{235} + l_4 + l_3s_{23} + l_2s_2 + l_1 \end{cases} \tag{14}$$

To solve for the center-of-mass velocity of each linkage, the center-of-mass coordinates of each link are derived separately, and the components of the center-of-mass velocity of each linkage in the three directions of the coordinate system can be obtained as

Link 1:

$$\begin{cases} \dot{x}_1 = 0 \\ \dot{y}_1 = 0 \\ \dot{z}_1 = 0 \end{cases} \tag{15}$$

Link 2:

$$\begin{cases} \dot{x}_2 = -\dfrac{1}{2}l_2s_2c_1\dot{\theta}_2 - \dfrac{1}{2}l_2c_2s_1\dot{\theta}_1 \\ \dot{y}_2 = -\dfrac{1}{2}l_2s_2s_1\dot{\theta}_2 + \dfrac{1}{2}l_2c_2c_1\dot{\theta}_1 \\ \dot{z}_2 = \dfrac{1}{2}l_2c_2\dot{\theta}_2 \end{cases} \tag{16}$$

Link 3:

$$\begin{cases} \dot{x}_3 = \left(-l_2s_2\dot{\theta}_2 - \dfrac{1}{2}l_3s_{23}\left(\dot{\theta}_2 + \dot{\theta}_3\right)\right)c_1 \\ \qquad - \left(l_2c_2 + \dfrac{1}{2}l_3c_{23}\right)s_1\dot{\theta}_1 \\ \dot{y}_3 = \left(-l_2s_2\dot{\theta}_2 - \dfrac{1}{2}l_3s_{23}\left(\dot{\theta}_2 + \dot{\theta}_3\right)\right)s_1 \\ \qquad + \left(l_2c_2 + \dfrac{1}{2}l_3c_{23}\right)c_1\dot{\theta}_1 \\ \dot{z}_3 = \dfrac{1}{2}l_3c_{23}\left(\dot{\theta}_2 + \dot{\theta}_3\right) + l_2c_2\dot{\theta}_2 \end{cases} \tag{17}$$

Link 4:

$$\begin{cases} \dot{x}_4 = \left(-l_2s_2\dot{\theta}_2 - \dfrac{1}{2}l_3s_{23}\left(\dot{\theta}_2 + \dot{\theta}_3\right)\right)c_1 \\ \qquad - \left(l_2c_2 + \dfrac{1}{2}l_3c_{23}\right)s_1\dot{\theta}_1 \\ \dot{y}_4 = \left(-l_2s_2\dot{\theta}_2 - \dfrac{1}{2}l_3s_{23}\left(\dot{\theta}_2 + \dot{\theta}_3\right)\right)s_1 \\ \qquad + \left(l_2c_2 + \dfrac{1}{2}l_3c_{23}\right)c_1\dot{\theta}_1 \\ \dot{z}_4 = l_3c_{23}\left(\dot{\theta}_2 + \dot{\theta}_3\right) + l_2c_2\dot{\theta}_2 \end{cases} \tag{18}$$

Link 5:

$$\begin{cases} \dot{x}_5 = \Big[- l_2s_2\dot{\theta}_2 - l_3s_{23}\left(\dot{\theta}_2 + \dot{\theta}_3\right) \\ \qquad - \dfrac{1}{2}l_5s_{235}\left(\dot{\theta}_2 + \dot{\theta}_3 + \dot{\theta}_5\right)\Big]c_1 \\ \qquad - \left(l_2c_2 + l_3c_{23} + \dfrac{1}{2}l_5c_{235}\right)s_1\dot{\theta}_1 \\ \dot{y}_5 = \Big[- l_2s_2\dot{\theta}_2 - l_3s_{23}\left(\dot{\theta}_2 + \dot{\theta}_3\right) \\ \qquad - \dfrac{1}{2}l_5s_{235}\left(\dot{\theta}_2 + \dot{\theta}_3 + \dot{\theta}_5\right)\Big]s_1 \\ \qquad + \left(l_2c_2 + l_3c_{23} + \dfrac{1}{2}l_5c_{235}\right)c_1\dot{\theta}_1 \\ \dot{z}_5 = \dfrac{l_5}{2}c_5\dot{\theta}_5 + l_3c_{23}\left(\dot{\theta}_2 + \dot{\theta}_3\right) + l_2c_2\dot{\theta}_2 \end{cases} \tag{19}$$

Link 6:

$$\begin{cases} \dot{x}_6 = \Big[- l_2s_2\dot{\theta}_2 - l_3s_{23}\left(\dot{\theta}_2 + \dot{\theta}_3\right) \\ \qquad - \dfrac{1}{2}l_5s_{235}\left(\dot{\theta}_2 + \dot{\theta}_3 + \dot{\theta}_5\right)\Big]c_1 \\ \qquad - \left(l_2c_2 + l_3c_{23} + \dfrac{1}{2}l_5c_{235}\right)s_1\dot{\theta}_1 \\ \dot{y}_6 = \Big[- l_2s_2\dot{\theta}_2 - l_3s_{23}\left(\dot{\theta}_2 + \dot{\theta}_3\right) \\ \qquad - \dfrac{1}{2}l_5s_{235}\left(\dot{\theta}_2 + \dot{\theta}_3 + \dot{\theta}_5\right)\Big]s_1 \\ \qquad + \left(l_2c_2 + l_3c_{23} + \dfrac{1}{2}l_5c_{235}\right)c_1\dot{\theta}_1 \\ \dot{z}_6 = l_5c_{235}\left(\dot{\theta}_2 + \dot{\theta}_3 + \dot{\theta}_5\right) + l_3c_{23}\left(\dot{\theta}_2 + \dot{\theta}_3\right) + l_2c_2\dot{\theta}_2 \end{cases} \tag{20}$$

Based on the velocity of each center of mass solved above, the specific expression for the kinetic energy of each link can now be found.

Link 1:

$$E_{k1} = \frac{1}{2}I_1\dot{\theta}_1^2 \tag{21}$$

Link 2:

$$\begin{aligned} E_{k2} &= \frac{m_2}{2}\left(\dot{x}_2^2 + \dot{y}_2^2 + \dot{z}_2^2\right) + \frac{1}{2}I_2\dot{\theta}_2^2 \\ &= \frac{m_2}{2}\left(\frac{1}{4}l_2^2\dot{\theta}_2^2 + \frac{1}{4}l_2^2c_2^2\dot{\theta}_1^2\right) + \frac{1}{2}I_2\dot{\theta}_2^2 \end{aligned} \tag{22}$$

Link 3:

$$\begin{aligned}E_{k3} &= \frac{m_3}{2}\left(\dot{x}_3^2+\dot{y}_3^2+\dot{z}_3^2\right)+\frac{1}{2}I_3\left(\dot{\theta}_2+\dot{\theta}_3\right)^2\\ &= \frac{m_3}{2}\left[l_2s_2\dot{\theta}_2+\frac{l_3}{2}s_{23}\left(\dot{\theta}_2+\dot{\theta}_3\right)\right]^2\\ &\quad+\frac{m_3}{2}\left(l_2c_2+\frac{l_3}{2}c_{23}\right)^2\dot{\theta}_1^2\\ &\quad+\frac{m_3}{2}\left[l_2c_2\dot{\theta}_2+\frac{l_3}{2}c_{23}\left(\dot{\theta}_2+\dot{\theta}_3\right)\right]^2+\frac{1}{2}I_3\left(\dot{\theta}_2+\dot{\theta}_3\right)^2\end{aligned} \tag{23}$$

Link 4:

$$\begin{aligned}E_{k4} &= \frac{m_4}{2}\left(\dot{x}_4^2+\dot{y}_4^2+\dot{z}_4^2\right)+\frac{1}{2}I_4\left(\dot{\theta}_1+\dot{\theta}_4\right)^2\\ &= \frac{m_4}{2}\left[l_2s_2\dot{\theta}_2+\frac{l_3}{2}s_{23}\left(\dot{\theta}_2+\dot{\theta}_3\right)\right]^2\\ &\quad+\frac{m_4}{2}\left(l_2c_2+\frac{l_3}{2}c_{23}\right)^2\dot{\theta}_1^2\\ &\quad+\frac{m_4}{2}\left[l_2c_2\dot{\theta}_2+l_3c_{23}\left(\dot{\theta}_2+\dot{\theta}_3\right)\right]^2+\frac{1}{2}I_4\left(\dot{\theta}_1+\dot{\theta}_4\right)^2\end{aligned} \tag{24}$$

Link 5:

$$\begin{aligned}E_{k5} &= \frac{m_5}{2}\left(\dot{x}_5^2+\dot{y}_5^2+\dot{z}_5^2\right)+\frac{1}{2}I_5\left(\dot{\theta}_2+\dot{\theta}_3+\dot{\theta}_5\right)^2\\ &= \frac{m_5}{2}\left[l_2s_2\dot{\theta}_2+l_3s_{23}\left(\dot{\theta}_2+\dot{\theta}_3\right)\right.\\ &\quad\left.+\frac{l_5}{2}s_{235}\left(\dot{\theta}_2+\dot{\theta}_3+\dot{\theta}_5\right)\right]^2\\ &\quad+\frac{1}{2}I_5\left(\dot{\theta}_2+\dot{\theta}_3+\dot{\theta}_5\right)^2\\ &\quad+\frac{m_5}{2}\left(l_2c_2+l_3c_{23}+\frac{l_5}{2}c_{235}\right)^2\dot{\theta}_1^2\\ &\quad+\frac{m_5}{2}\left[l_2c_2\dot{\theta}_2+l_3c_{23}\left(\dot{\theta}_2+\dot{\theta}_3\right)+\frac{l_5}{2}c_5\dot{\theta}_5\right]^2\end{aligned} \tag{25}$$

Link 6:

$$\begin{aligned}E_{k6} &= \frac{m_6}{2}\left(\dot{x}_6^2+\dot{y}_6^2+\dot{z}_6^2\right)+\frac{1}{2}I_6\left(\dot{\theta}_1+\dot{\theta}_4+\dot{\theta}_6\right)^2\\ &= \frac{m_6}{2}\left[l_2s_2\dot{\theta}_2+l_3s_{23}\left(\dot{\theta}_2+\dot{\theta}_3\right)+\frac{l_5}{2}s_{235}\left(\dot{\theta}_2+\dot{\theta}_3+\dot{\theta}_5\right)\right]^2\\ &\quad+\frac{m_6}{2}\left[l_2c_2\dot{\theta}_2+l_3c_{23}\left(\dot{\theta}_2+\dot{\theta}_3\right)+l_5c_{235}\left(\dot{\theta}_2+\dot{\theta}_3+\dot{\theta}_5\right)\right]^2\\ &\quad+\frac{m_6}{2}\left(l_2c_2+l_3c_{23}+\frac{l_5}{2}c_{235}\right)^2\dot{\theta}_1^2\\ &\quad+\frac{1}{2}I_6\left(\dot{\theta}_1+\dot{\theta}_4+\dot{\theta}_6\right)^2\end{aligned} \tag{26}$$

B. SOLVING FOR POTENTIAL ENERGY OF SYSTEM

Based on the coordinates of the center of mass of the link obtained in the previous section, we can find the gravitational potential energy of each link separately.

Link 1:

$$E_{p1} = \frac{l_1}{2}m_1g \tag{27}$$

Link 2:

$$E_{p2} = m_2g\left(l_1+\frac{l_2}{2}s_2\right) \tag{28}$$

Link 3:

$$E_{p3} = m_3g\left(l_1+l_2s_2+\frac{l_3}{2}s_{23}\right) \tag{29}$$

Link 4:

$$E_{p4} = m_4g\left(l_1+l_2s_2+l_3s_{23}+\frac{l_4}{2}\right) \tag{30}$$

Link 5:

$$E_{p5} = m_5g\left(l_1+l_2s_2+l_3s_{23}+l_4+\frac{l_5}{2}s_{235}\right) \tag{31}$$

Link 6:

$$E_{p6} = m_6g\left(l_1+l_2s_2+l_3s_{23}+l_4+l_5s_{235}+\frac{l_6}{2}\right) \tag{32}$$

C. SOLUTION FOR SYSTEM DYNAMICS EQUATION

Based on the kinetic and potential energies of each linkage obtained in Sections *A* and *B*, the detailed Lagrange function of the P-Rob six-degree-of-freedom robot manipulator can now be obtained

$$L = \sum_{i=1}^{6}E_{ki}-\sum_{i=1}^{6}E_{pi} \tag{33}$$

The obtained Lagrange functions are derived separately for the system state and time, which leads to the dynamics equations for the six joints.

1) SOLUTION OF THE 1ST DYNAMICS EQUATION

Taking the partial derivative of $\dot{\theta}_1$ in the Lagrange function yields

$$\begin{aligned}\frac{\partial L}{\partial\dot{\theta}_1} &= \left(I_1+I_4+I_6+\frac{m_2}{4}l_2^2c_2^2+(m_3+m_4)\right.\\ &\quad\left.\times\left(l_2c_2+\frac{l_3}{2}c_{23}\right)^2\right)\dot{\theta}_1\\ &\quad+(m_5+m_6)\left(l_2c_2+l_3c_{23}+\frac{l_5}{2}c_{235}\right)^2\dot{\theta}_1\\ &\quad+(I_4+I_6)\dot{\theta}_4+I_6\dot{\theta}_6\end{aligned} \tag{34}$$

The derivation of the above formula concerning time t can be obtained as

$$\begin{aligned}\frac{d}{dt}\frac{\partial L}{\partial\dot{\theta}_1} &= w_1\ddot{\theta}_1-w_2\dot{\theta}_1\dot{\theta}_2-(w_{15}+w_{16})\dot{\theta}_1\dot{\theta}_3\\ &\quad-w_{17}\dot{\theta}_1\dot{\theta}_5+(I_4+I_6)\ddot{\theta}_4+I_6\ddot{\theta}_6\end{aligned} \tag{35}$$

The coefficients of each item in the formula are expressed as

$$
\begin{aligned}
w_1 &= w_{11} + w_{12} + I_1 + I_4 + I_6 \\
w_2 &= \frac{m_2}{2} l_2^2 c_2 s_2 + w_{13} + w_{14} \\
w_{11} &= \frac{1}{4} m_2 l_2^2 c_2^2 + (m_3 + m_4) \left(l_2 c_2 + \frac{l_3}{2} c_{23} \right)^2 \\
w_{12} &= (m_5 + m_6) \left(l_2 c_2 + l_3 c_{23} + \frac{l_5}{2} c_{235} \right)^2 \\
w_{13} &= \left(l_2 s_2 + \frac{l_3}{2} s_{23} \right) (2 l_2 c_2 + l_2 c_{23}) (m_3 + m_4) \\
w_{14} &= \left(l_2 s_2 + l_3 s_{23} + \frac{l_5}{2} s_{235} \right) (2 l_2 c_2 + 2 l_3 c_{23} + l_5 c_{235}) \\
&\quad \times (m_5 + m_6) \\
w_{15} &= \frac{l_3}{2} s_{23} (2 l_2 c_2 + l_2 c_{23}) (m_3 + m_4) \\
w_{16} &= \left(l_3 s_{23} + \frac{l_5}{2} s_{235} \right) (2 l_2 c_2 + 2 l_3 c_{23} + l_5 c_{235}) \\
&\quad \times (m_5 + m_6) \\
w_{17} &= \frac{l_5}{2} s_{235} (2 l_2 c_2 + 2 l_3 c_{23} + l_5 c_{235}) (m_5 + m_6)
\end{aligned}
$$

Taking the partial derivative of θ_1 in the Lagrange function yields

$$\frac{\partial L}{\partial \theta_1} = 0 \tag{36}$$

According to (35) and (36) and considering the existence of disturbance d_1 in the system, the first dynamics equations can be obtained

$$\tau_1 + d_1 = \frac{d}{dt} \frac{\partial L}{\partial \dot{\theta}_1} - \frac{\partial L}{\partial \theta_1} \tag{37}$$

2) SOLUTION OF THE 2ND DYNAMICS EQUATIONS

Taking the partial derivative of $\dot{\theta}_2$ in the Lagrange function yields

$$\frac{\partial L}{\partial \dot{\theta}_2} = (f_1 + f_2 + f_3) \dot{\theta}_2 + (f_4 + f_5 + f_6) \dot{\theta}_3 + (f_7 + f_8) \dot{\theta}_5 \tag{38}$$

The coefficients of each item in the formula are expressed as

$$
\begin{aligned}
f_1 &= I_2 + I_3 + I_5 + \frac{m_2}{4} l_2^2 c_2^2 \\
&\quad + (m_3 + m_4) \left(l_2 s_2 + \frac{l_3}{2} s_{23} \right) \left(l_2 c_2 + \frac{l_3}{2} s_{23} \right) \\
f_2 &= (m_5 + m_6) \left(l_2 s_2 + l_3 s_{23} + \frac{l_5}{2} s_{235} \right)^2 \\
&\quad + m_6 (l_5 c_{235} + l_3 c_{23} + l_2 c_2)^2 \\
f_3 &= m_3 \left(l_2 c_2 + \frac{l_3}{2} c_{23} \right)^2 + m_4 (l_3 c_{23} + l_2 c_2)^2 \\
&\quad + m_5 (l_3 c_{23} + l_2 c_2)^2 \\
f_4 &= I_3 + I_5 + \frac{(m_3 + m_4) l_3 s_{23}}{2} \left(l_2 s_2 + \frac{l_3}{2} s_{23} \right) \\
&\quad + \frac{m_3 l_3 c_{23}}{2} \left(l_2 c_2 + \frac{l_3}{2} c_{23} \right) \\
f_5 &= m_4 l_3 c_{23} (l_3 c_{23} + l_2 c_2) \\
&\quad + (m_5 + m_6) \left(l_2 s_2 + l_3 s_{23} + \frac{l_5}{2} s_{235} \right) \left(l_3 s_{23} + \frac{l_5}{2} s_{235} \right) \\
f_6 &= m_5 l_3 c_{23} (l_3 c_{23} + l_2 c_2) \\
&\quad + m_6 (l_5 c_{235} + l_3 c_{23} + l_2 c_2) (l_5 c_{235} + l_3 c_{23}) \\
f_7 &= I_5 + \frac{(m_5 + m_6) l_5 s_{235}}{2} \left(l_2 s_2 + l_3 s_{23} + \frac{l_5}{2} s_{235} \right) \\
f_8 &= \frac{m_5 l_5 c_5}{2} (l_3 c_{23} + l_2 c_2) + m_6 l_5 c_{235} (l_5 c_{235} + l_3 c_{23} + l_2 c_2)
\end{aligned}
$$

Derivation of the above formula concerning time t can be obtained as

$$
\begin{aligned}
\frac{d}{dt} \frac{\partial L}{\partial \dot{\theta}_2} &= q_1 \dot{\theta}_2^2 + q_2 \dot{\theta}_3^2 + q_3 \dot{\theta}_5^2 + q_4 \dot{\theta}_2 \dot{\theta}_3 + q_5 \dot{\theta}_2 \dot{\theta}_5 \\
&\quad + q_6 \dot{\theta}_3 \dot{\theta}_5 + q_7 \ddot{\theta}_2 + q_8 \ddot{\theta}_3 + q_9 \ddot{\theta}_5
\end{aligned} \tag{39}
$$

The coefficients of each item in the formula are expressed as

$$
\begin{aligned}
q_1 &= (m_3 + m_4) \left(l_2^2 c_2^2 - l_2^2 s_2^2 + \frac{l_3^2 s_{23}^2}{4} - \frac{l_2 l_3 s_2 s_{23}}{2} \right) \\
&\quad + (m_5 - m_6) l_3 l_5 \sin(2\theta_2 + 2\theta_3 + \theta_5) - \frac{7 m_4 l_3^2 c_{23} s_{23}}{4} \\
&\quad - \left(\frac{m_2}{2} + 2m_3 + 2m_4 \right) l_2^2 c_2 s_2 + \left(\frac{m_5 - 3m_6}{2} \right) \frac{l_5^2}{2} c_{235} s_{235} \\
&\quad - \left(\frac{m_3 + 3m_4}{2} \right) l_2 l_3 s_2 c_{23} - m_4 l_2 l_3 c_2 s_{23} \\
&\quad + (m_5 + m_6) l_2 l_5 \sin(2\theta_2 + \theta_3 + \theta_5) \\
q_2 &= (m_3 + m_4) \left(\frac{l_3^2 s_{23}^2 + l_3^2 s_{23} + 2 l_2 l_3 s_2}{4} \right) - m_6 l_2 l_3 c_2 s_{235} \\
&\quad + (m_5 + m_6) \left(\frac{l_2 l_5 s_2 c_{235}}{2} - l_2 l_3 s_3 \right) \\
&\quad + \left(\frac{m_5}{2} - m_6 \right) l_3 l_5 c_{23} s_{235} \\
&\quad - \left(\frac{m_3}{2} + 2m_4 \right) l_3^2 c_{23} s_{23} - \left(\frac{m_3}{2} + m_4 \right) l_2 l_3 c_2 s_{23} \\
&\quad + (m_5 - m_6) l_3 l_5 c_{23} s_{235} + \left(\frac{m_5 - 3m_6}{2} \right) l_5^2 c_{235} s_{235} \\
q_3 &= (m_5 - 3m_6) \frac{l_5^2}{2} c_{235} s_{235} + (m_5 + m_6) \\
&\quad \times \frac{l_5 c_{235}}{2} (l_2 s_2 + l_3 s_{23}) \\
&\quad - \left(\frac{m_5 s_5}{2} + m_6 s_{235} \right) l_5 (l_3 c_{23} + l_2 c_2) \\
q_4 &= (m_3 + m_4) \frac{l_3^2}{2} s_{23}^2 - \frac{m_3 l_2 l_3 s_3}{2} - (m_3 + 7m_4) \frac{l_3^2 c_{23} s_{23}}{2} \\
&\quad + 2 l_3 c_{23} (m_5 + m_6) (l_2 s_2 - l_3 s_{23}) \\
&\quad - (3m_5 + 4m_6) l_2 l_3 c_2 s_{23} \\
&\quad + (m_5 - 3m_6) l_3 l_5 \sin(2\theta_2 + 2\theta_3 + \theta_5) - 2 m_4 l_2 l_3 c_2 s_{23} \\
&\quad + (3m_5 + m_6) \frac{l_2 l_5 s_2 c_{235}}{2} - (m_5 + 7m_6) \frac{l_2 l_5 c_2 s_{235}}{2}
\end{aligned}
$$

$$
\begin{aligned}
&+ (m_5 - 7m_6)\frac{l_5^2 s_{235}c_{235}}{2} - m_5 l_2 l_5 c_2 s_{23}\\
q_5 &= (m_5 - 5m_6)\frac{l_5 s_{235}}{2}(l_2 c_2 + l_3 c_{23})\\
&+ (3m_5 + m_6)\frac{l_5 c_{235}}{2}(l_2 s_2 + l_3 s_{23})\\
&- \frac{m_5 l_5 c_5}{2}(l_2 s_2 - l_3 s_{23}) + (m_5 - 3m_6) l_5^2 c_{235} s_{235}\\
q_6 &= (m_5 - 5m_6)\frac{l_3 l_5}{2} c_{23} s_{235} + (3m_5 + m_6)\frac{l_3 l_5}{2} s_{23} c_{235}\\
&+ (m_5 - 3m_6) l_5^2 c_{235} s_{235} - \frac{m_5 l_3 l_5}{2} c_5 s_{23}\\
&- 2m_6 l_2 l_5 c_2 s_{235} + (m_5 + m_6) l_2 l_5 s_2 c_{235}\\
q_7 &= \frac{m_2 l_2^2 c_2^2}{4} + (m_3 + m_4)\\
&\times \left(l_2^2 c_2^2 + l_2^2 c_2 s_2 + \frac{l_2 l_3 s_2 s_{23}}{2} + \frac{l_2 l_3 c_2 s_{23}}{2}\right)\\
&+ \frac{m_3 l_3^2}{4} + m_4 l_3^2\left(\frac{s_{23}^2}{4} + c_{23}^2\right) + m_6 l_5 c_{235}\\
&\times (2l_2 c_2 + 2l_3 c_{23} + l_5 c_{235}) + (m_5 + m_6)\\
&\times \left(l_2^2 + 2l_2 l_3 c_3 + l_3^2 + l_2 l_5 s_2 s_{235} + l_3 l_5 s_{23} s_{235} + \frac{l_5^2 s_{235}^2}{4}\right)\\
&+ (m_3 + 2m_4) l_2 l_3 c_2 c_{23} + I_2 + I_3 + I_5\\
q_8 &= (m_3 + m_4)\left(\frac{l_2 l_3 s_2 s_{23}}{2} + \frac{l_3^2 s_{23}^2}{4}\right)\\
&+ \left(\frac{m_3}{2} + m_4\right) l_2 l_3 c_2 c_{23} + (m_5 + m_6)\\
&\times \left(l_2 l_3 c_3 + l_3^2 + l_3 l_5 s_{23} s_{235} + \frac{l_2 l_5}{2} s_2 s_{235} + \frac{l_5^2 s_{235}^2}{4}\right)\\
&+ \left(\frac{m_3}{4} + m_4\right) l_3^2 c_{23}^2 + m_6 l_5 c_{235}\\
&\times (l_2 c_2 + 2l_3 c_{23} + l_5 c_{235}) + I_3 + I_5\\
q_9 &= (m_5 + m_6)\frac{l_5 s_{235}}{2}\left(l_2 s_2 + l_3 s_{23} + \frac{l_5 s_{235}}{2}\right)\\
&+ \frac{m_5 l_5 c_5}{2}(l_3 c_{23} + l_2 c_2) + m_6 l_5 c_{235}\\
&\times (l_2 c_2 + l_3 c_{23} + l_5 c_{235}) + I_5
\end{aligned}
$$

Taking the partial derivative of θ_2 in the Lagrange function yields

$$
\begin{aligned}
\frac{\partial L}{\partial \theta_2} &= -a_1\dot{\theta}_1^2 + a_2\dot{\theta}_2^2 + a_3\dot{\theta}_3^2 + a_4\dot{\theta}_5^2\\
&+ a_5\dot{\theta}_2\dot{\theta}_3 + a_6\dot{\theta}_2\dot{\theta}_5 + a_7\dot{\theta}_3\dot{\theta}_5\\
&- \frac{m_2 g}{2} l_2 c_2 - m_3 g\left(l_2 c_2 + \frac{l_3}{2} c_{23}\right)\\
&- m_4 g (l_2 c_2 + l_3 c_{23})\\
&- m_5 g\left(l_2 c_2 + l_3 c_{23} + \frac{l_5}{2} c_{235}\right)\\
&- m_6 g (l_2 c_2 + l_3 c_{23} + l_5 c_{235})
\end{aligned} \tag{40}
$$

The coefficients of each item in the formula are expressed as

$$
\begin{aligned}
a_1 &= \frac{m_2}{4} l_2^2 c_2 s_2 + a_{11}(m_3 + m_4) + a_{19}(m_5 + m_6)\\
a_2 &= a_{14} m_5 - a_{12} m_4 - a_{20} m_6\\
a_3 &= a_{15} m_5 - a_{21} m_6 - \frac{3}{4} m_4 l_2^2 c_{23} s_{23}\\
a_4 &= \frac{m_5 l_5^2}{2} s_{23} - \frac{3}{4} m_6 l_5^2 c_{235} s_{235}\\
a_5 &= a_{16} m_5 - a_{13} m_4 - a_{22} m_6\\
a_6 &= a_{17} m_5 - a_{23} m_6\\
a_7 &= a_{18} m_5 - a_{24} m_6\\
a_{11} &= \left(l_2 c_2 + \frac{l_3}{2} c_{23}\right)\left(l_2 s_2 + \frac{l_3}{2} s_{23}\right)\\
a_{12} &= \frac{3}{4} c_{23} s_{23} + \frac{l_2 l_3}{2}\sin(2\theta_2 + \theta_3)\\
a_{13} &= \frac{3}{2} l_3^2 c_{23} s_{23} + \frac{l_2 l_3}{2}\sin(2\theta_2 + \theta_3)\\
a_{14} &= \frac{l_5^2}{2} c_{235} s_{235} + \frac{l_2 l_5}{2}\sin(2\theta_2 + \theta_3 + \theta_5)\\
&+ \frac{l_2 l_5}{2}\sin(2\theta_2 + 2\theta_3 + \theta_5)\\
a_{15} &= \frac{l_5^2}{4} c_{235} s_{235} + \frac{l_3 l_5}{2}\sin(2\theta_2 + 2\theta_3 + \theta_5)\\
a_{16} &= \frac{l_5^2}{2} c_{235} s_{235} + \frac{l_2 l_5}{2}\sin(2\theta_2 + \theta_3 + \theta_5)\\
&+ l_3 l_5 \sin(2\theta_2 + 2\theta_3 + \theta_5)\\
a_{17} &= \frac{l_5^2}{2} c_{235} s_{235} + \frac{l_2 l_5}{2}[\sin(2\theta_2 + \theta_3 + \theta_5) - s_{25}]\\
&+ \frac{l_3 l_5}{2}[\sin(2\theta_2 + 2\theta_3 + \theta_5) - s_{235}]\\
a_{18} &= \frac{l_5^2}{2} c_{235} s_{235} + \frac{l_3 l_5}{2}\sin(2\theta_2 + 2\theta_3 + \theta_5)\\
a_{19} &= \left(l_2 c_2 + l_3 c_{23} + \frac{l_5}{2} c_{235}\right)\left(l_2 s_2 + l_3 s_{23} + \frac{l_5}{2} s_{235}\right)\\
a_{20} &= \frac{3l_5^2}{4} c_{235} s_{235} + \frac{l_2 l_5}{2}\sin(2\theta_2 + \theta_3 + \theta_5)\\
&+ \frac{l_3 l_5}{2}\sin(2\theta_2 + 2\theta_3 + \theta_5)\\
a_{21} &= \frac{3l_5^2}{4} c_{235} s_{235} + \frac{l_3 l_5}{2}\sin(2\theta_2 + 2\theta_3 + \theta_5)\\
a_{22} &= \frac{3l_5^2}{2} c_{235} s_{235} + \frac{l_2 l_5}{2}\sin(2\theta_2 + \theta_3 + \theta_5)\\
&+ l_3 l_5 \sin(2\theta_2 + 2\theta_3 + \theta_5)\\
a_{23} &= \frac{3l_5^2}{2} c_{235} s_{235} + \frac{l_2 l_5}{2}\sin(2\theta_2 + \theta_3 + \theta_5)\\
&+ \frac{l_3 l_5}{2}\sin(2\theta_2 + 2\theta_3 + \theta_5)\\
a_{24} &= \frac{3l_5^2}{4} c_{235} s_{235} + \frac{l_3 l_5}{2}\sin(2\theta_2 + 2\theta_3 + \theta_5)
\end{aligned}
$$

According to (39) and (40) and considering the existence of disturbance d_2 in the system, the second dynamics equations can be obtained:

$$\tau_2 + d_2 = \frac{d}{dt}\frac{\partial L}{\partial \dot{\theta}_2} - \frac{\partial L}{\partial \theta_2} \tag{41}$$

3) SOLUTION OF THE 3RD DYNAMICS EQUATIONS

Taking the partial derivative of $\dot{\theta}_3$ in the Lagrange function yields

$$\frac{\partial L}{\partial \dot{\theta}_3} = (r_1 + r_2 + r_3)\,\dot{\theta}_2 + (r_4 + r_5)\,\dot{\theta}_3 + r_6\dot{\theta}_5 \tag{42}$$

The coefficients of each item in the formula are expressed as

$$\begin{aligned}
r_1 &= I_3 + I_5 + \frac{(m_3+m_4)}{2} l_3 s_{23}\left(l_2 s_2 + \frac{l_3}{2} s_{23}\right) \\
&\quad + \frac{m_3}{2} l_3 c_{23}\left(\frac{l_3}{2} c_{23} + l_2 c_2\right) \\
r_2 &= (m_5+m_6)\left(l_3 s_{23} + \frac{l_5}{2} s_{235}\right)\left(l_2 s_2 + l_3 s_{23} + \frac{l_5}{2} s_{235}\right) \\
r_3 &= (m_4+m_5)\, l_3 c_{23}\,(l_3 c_{23} + l_2 c_2) \\
&\quad + m_6\,(l_5 c_{235} + l_3 c_{23})\,(l_5 c_{235} + l_3 c_{23} + l_2 c_2) \\
r_4 &= I_3 + I_5 + \frac{(m_3+m_4)\, l_3^2 s_{23}^2}{4} \\
&\quad + (m_5+m_6)\left(l_3 s_{23} + \frac{l_5}{2} s_{235}\right)^2 \\
r_5 &= \frac{m_3 l_3^2 c_{23}^2}{4} + (m_4+m_5)\, l_3^2 c_{23}^2 + m_6\,(l_5 c_{235} + l_3 c_{23})^2 \\
r_6 &= I_5 + \frac{(m_5+m_6)\, l_5 s_{235}}{2}\left(l_3 s_{23} + \frac{l_5}{2} s_{235}\right) \\
&\quad + \frac{m_5 l_3 l_5 c_{23} c_5}{2} + m_6 l_5 c_{235}\,(l_5 c_{235} + l_3 c_{23})
\end{aligned}$$

Derivation of the above formula concerning time t can be obtained as

$$\begin{aligned}
\frac{d}{dt}\frac{\partial L}{\partial \dot{\theta}_3} &= j_1\dot{\theta}_2^2 + j_2\dot{\theta}_3^2 + j_3\dot{\theta}_5^2 + j_4\dot{\theta}_2\dot{\theta}_3 \\
&\quad + j_5\dot{\theta}_2\dot{\theta}_5 + j_6\dot{\theta}_3\dot{\theta}_5 + j_7\ddot{\theta}_2 + j_8\ddot{\theta}_3 + j_9\ddot{\theta}_5
\end{aligned} \tag{43}$$

The coefficients of each item in the formula are expressed as

$$\begin{aligned}
j_1 &= \frac{m_3+m_4}{2} l_3^2 c_2 s_{23} - \left(\frac{m_3}{2} + m_4\right) l_2 l_3 c_2 s_{23} \\
&\quad - \frac{m_4}{2} l_2 l_3 s_2 c_{23} \\
&\quad + \left(m_5 - \frac{3m_4}{2}\right) l_3^2 c_{23} s_{23} + \frac{m_5 - m_6}{2} l_2 l_5 s_2 c_{235} \\
&\quad - m_5 l_3 l_5 c_{23} s_{23} \\
&\quad + (m_5 - m_6)\, l_3 l_5 \sin(2\theta_2 + 2\theta_3 + \theta_5) \\
&\quad + \left(\frac{m_5}{2} - m_6\right) l_2 l_5 c_2 s_{235} \\
&\quad + \left(\frac{m_5}{2} - 2m_6\right) l_5^2 c_{235} s_{235} + (l_3 - l_5)\, m_5 l_2 c_2 s_{23} \\
j_2 &= \left(m_5 l_3^2 - \frac{3}{2} m_4 l_3^2 - m_5 l_3 l_5\right) c_{23} s_{23} \\
&\quad + (m_5 - 3m_6)\, \frac{l_5^2}{2} c_{235} s_{235} \\
&\quad + \left(m_5 - \frac{3}{2} m_6\right) l_3 l_5 \sin(2\theta_2 + 2\theta_3 + \theta_5) \\
j_3 &= (m_5+m_6)\, \frac{l_3 l_5}{2} s_{23} c_{235} + \frac{l_5^2}{2}(m_5 - 3m_6)\, s_{235} c_{235} \\
&\quad - \frac{m_5 l_3 l_5}{2} s_5 c_{23} - m_6 l_3 l_5 c_{23} s_{235} \\
j_4 &= (2m_5 l_3 - 3m_4 l_3 - 2m_5 l_5)\, l_3 c_{23} s_{23} \\
&\quad - \left(\frac{m_3}{2} + m_6\right) l_2 l_3 s_3 \\
&\quad + 2 l_3 l_5\,(m_5 - m_6) \sin(2\theta_2 + 2\theta_3 + \theta_5) + m_5 l_2 l_3 s_2 c_{23} \\
&\quad + m_4 l_2 l_3 \left(\frac{s_2 c_{23}}{2} - c_2 s_{23}\right) + (m_5 - 3m_6)\, l_5^2 c_{235} s_{235} \\
&\quad + \frac{m_5}{2} l_2 l_5 s_2 c_{235} - m_5 l_2 l_5 c_2 s_{23} \\
&\quad + m_6 l_2 l_5 \left(\frac{s_2 c_{235}}{2} - c_2 s_{235}\right) \\
j_5 &= (m_5 - 5m_6)\, \frac{l_3 l_5}{2} c_{23} s_{235} + (m_5 - 3m_6)\, l_5^2 c_{235} s_{235} \\
&\quad + (m_5+m_6)\, \frac{l_2 l_5}{2} s_2 c_{235} - \frac{m_5}{2} l_5^2 s_{23} c_5 - m_6 l_2 l_5 c_2 s_{235} \\
&\quad + (3m_5 + m_6)\, \frac{l_3 l_5}{2} s_{23} c_{235} \\
j_6 &= (m_5 - m_6)\left(l_5^2 c_{235} s_{235} + \frac{l_3 l_5}{2} c_{23} s_{235}\right) \\
&\quad + (3m_5 + m_6)\, \frac{l_3 l_5}{2} s_{23} c_{235} - \frac{m_5 l_5^2}{2} s_{23} c_5 - 2m_6 l_5 s_{235} \\
j_7 &= (m_3+m_4)\left(\frac{l_2 l_3 s_2 s_{23}}{2} + \frac{l_3^2 s_{23}^2}{4}\right) \\
&\quad + \left(\frac{m_3}{2} + m_4\right) l_2 l_3 c_2 c_{23} + I_3 + \left(\frac{m_3}{4} + m_4\right) l_3^2 c_{23}^2 \\
&\quad + m_6 l_5 c_{235}\,(l_2 c_2 + 2 l_3 c_{23} + l_5 c_{235}) + I_5 + (m_5+m_6) \\
&\quad \times \left(l_2 l_3 c_3 + l_3^2 + l_3 l_5 s_{23} s_{235} + \frac{l_2 l_5}{2} s_2 s_{235} + \frac{l_5^2 s_{235}^2}{4}\right) \\
j_8 &= \left(\frac{m_3+m_4}{4}\right) l_3^2 s_{23}^2 + \left(\frac{m_3}{4} + m_4\right) l_3^2 c_{23}^2 + m_6 l_5^2 c_{235}^2 \\
&\quad + 2 m_6 l_3 l_5 c_{23} c_{235} + (m_5+m_6) \\
&\quad \times \left(l_3^2 + \frac{l_5^2 s_{235}^2}{4} + l_3 l_5 s_{23} s_{235}\right) \\
j_9 &= (m_5+m_6)\left(\frac{l_3 l_5}{2} s_{23} s_{235} + \frac{l_5^2}{4} s_{235}^2\right) + \frac{m_5 l_3 l_5}{2} c_5 c_{23} \\
&\quad + m_6\left(l_5^2 c_{235}^2 + l_3 l_5 c_{23} c_{235}\right) + I_5
\end{aligned}$$

Taking the partial derivative of θ_3 in the Lagrange function yields

$$\begin{aligned}
\frac{\partial L}{\partial \theta_3} &= b_1\dot{\theta}_1^2 + b_2\dot{\theta}_2^2 + b_3\dot{\theta}_3^2 + b_4\dot{\theta}_5^2 + b_5\dot{\theta}_2\dot{\theta}_3 + b_6\dot{\theta}_2\dot{\theta}_5 \\
&\quad + b_7\dot{\theta}_3\dot{\theta}_5 - \frac{l_3}{2} m_3 g c_{23} - m_5 g\left(l_3 c_{23} + \frac{l_5}{2} c_{235}\right) \\
&\quad - m_4 g l_3 c_{23} - m_6 g\,(l_3 c_{23} + l_5 c_{235})
\end{aligned} \tag{44}$$

The coefficients of each item in the formula are expressed as

$$
\begin{aligned}
b_1 &= -\left(m_3 + m_4\frac{l_3}{2}s_{23}\right)\left(l_2c_2 + \frac{l_3c_{23}}{2}\right) \\
&\quad \left(l_2c_2 + l_3c_{23} + \frac{l_5}{2}c_{235}\right)\left(l_3s_{23} + \frac{l_5s_{235}}{2}\right)(m_5 - m_6) \\
b_2 &= m_4\left[l_2l_3\left(\frac{s_2c_{23}}{2} - c_2s_{23}\right) - \frac{3}{4}l_3^2c_{23}s_{23}\right] \\
&\quad + (m_6 - m_5)\frac{l_2l_5s_2c_{235}}{2} - \frac{m_3l_2l_3s_2}{2} - m_6l_2l_5c_2s_{235} \\
&\quad (m_6 + m_5)\left[l_2l_3s_3 + \frac{l_3l_5}{2}\sin(2\theta_2 + 2\theta_3 + \theta_5)\right] \\
&\quad \frac{l_5^2}{4}s_{235}c_{235}(3m_6 + m_5) \\
b_3 &= -\frac{3}{4}m_4l_3^2c_{23}s_{23} + \frac{l_5^2}{4}(m_5 - 3m_6) \\
&\quad + \frac{l_3l_5}{2}(m_5 - m_6)\sin(2\theta_2 + 2\theta_3 + \theta_5) \\
b_4 &= s_{235}c_{235}\left(\frac{m_5l_5^2}{4} - \frac{3m_6l_5^2}{4}\right) \\
b_5 &= m_4\left[l_2l_3\left(\frac{s_2c_{23}}{2} - c_2s_{23}\right) - \frac{3l_3^2s_{23}c_{25}}{2}\right] \\
&\quad - m_6l_2l_5c_2s_{235} + (m_5 - m_6)l_3l_5\sin(2\theta_2 + 2\theta_3 + \theta_5) \\
&\quad - \frac{m_3l_2l_3s_3}{2} + (m_5 + m_6)\left(\frac{l_2l_5s_2c_{235}}{2} - l_2l_3s_3\right) \\
&\quad + (m_5 - 3m_6)\frac{l_5^2}{2}c_{235}s_{235} \\
b_6 &= \frac{l_2l_5}{2}(m_5 + m_6)s_2c_{235} - m_6l_2l_5c_2s_{235} \\
&\quad - \frac{m_5l_3l_5}{2}c_5s_{23} + (m_5 - 3m_6)\frac{l_5^2}{2}s_{235}c_{235} \\
&\quad + (m_5 - m_6)\frac{l_3l_5}{2}\sin(2\theta_2 + 2\theta_3 + \theta_5) \\
b_7 &= (m_5 - m_6)\frac{l_3l_5}{2}\sin(2\theta_2 + 2\theta_3 + \theta_5) \\
&\quad + (m_5 - 3m_6)\frac{l_5^2}{2}s_{235}c_{235} - \frac{m_5l_3l_5}{2}c_5s_{23}
\end{aligned}
$$

According to (43) and (44) and considering the existence of disturbance d_3 in the system, the third dynamics equation can be obtained as

$$\tau_3 + d_3 = \frac{d}{dt}\frac{\partial L}{\partial \dot{\theta}_3} - \frac{\partial L}{\partial \theta_3} \tag{45}$$

4) SOLUTION OF THE 4TH DYNAMICS EQUATIONS

Taking the partial derivative of $\dot{\theta}_4$ in the Lagrange function yields

$$\frac{\partial L}{\partial \dot{\theta}_4} = I_4\left(\dot{\theta}_1 + \dot{\theta}_4\right) + I_6\left(\dot{\theta}_1 + \dot{\theta}_4 + \dot{\theta}_6\right) \tag{46}$$

Derivation of the above formula concerning time t can be obtained as

$$\frac{d}{dt}\frac{\partial L}{\partial \dot{\theta}_4} = (I_4 + I_6)\ddot{\theta}_1 + (I_4 + I_6)\ddot{\theta}_4 + I_6\ddot{\theta}_6 \tag{47}$$

Taking the partial derivative of θ_4 in the Lagrange function yields

$$\frac{\partial L}{\partial \theta_4} = 0 \tag{48}$$

According to (47) and (48) and considering the existence of disturbance d_4 in the system, the fourth dynamics equation can be obtained as

$$\tau_4 + d_4 = \frac{d}{dt}\frac{\partial L}{\partial \dot{\theta}_4} - \frac{\partial L}{\partial \theta_4} \tag{49}$$

5) SOLUTION OF THE 5TH DYNAMICS EQUATIONS

Taking the partial derivative of $\dot{\theta}_5$ in the Lagrange function yields

$$
\begin{aligned}
\frac{\partial L}{\partial \dot{\theta}_5} &= \frac{(m_5 + m_6)}{2}l_5s_{235} \\
&\quad \times \left[l_2s_2\dot{\theta}_2 + l_3s_{23}\left(\dot{\theta}_2 + \dot{\theta}_3\right) + \frac{l_5}{2}s_{235}\left(\dot{\theta}_2 + \dot{\theta}_3 + \dot{\theta}_5\right)\right] \\
&\quad + I_5\left(\dot{\theta}_2 + \dot{\theta}_3 + \dot{\theta}_5\right) + \frac{m_5}{2}l_5c_5 \\
&\quad \times \left[\frac{l_5}{2}c_5\dot{\theta}_5 + l_3c_{23}\left(\dot{\theta}_2 + \dot{\theta}_3\right) + l_2c_2\dot{\theta}_2\right] \\
&\quad + m_6l_5c_{235}\left[l_5c_{235}\left(\dot{\theta}_2 + \dot{\theta}_3 + \dot{\theta}_5\right)\right. \\
&\quad \left. + l_3c_{23}\left(\dot{\theta}_2 + \dot{\theta}_3\right) + l_2c_2\dot{\theta}_2\right]
\end{aligned} \tag{50}
$$

Derivation of the above formula concerning time t can be obtained as

$$
\begin{aligned}
\frac{d}{dt}\frac{\partial L}{\partial \dot{\theta}_5} &= p_1\dot{\theta}_2^2 + p_2\dot{\theta}_2\dot{\theta}_3 + p_3\dot{\theta}_2\dot{\theta}_5 + p_4\dot{\theta}_3^2 + p_5\dot{\theta}_3\dot{\theta}_5 \\
&\quad + p_6\dot{\theta}_5^2 + p_7\ddot{\theta}_2 + p_8\ddot{\theta}_3 + p_9\ddot{\theta}_5
\end{aligned} \tag{51}
$$

The coefficients of each item in the formula are expressed as

$$
\begin{aligned}
p_1 &= p_{11} + p_{17} - s_{235}p_{14} - p_{18} \\
p_2 &= p_{11} + p_{12} + p_{19} + m_5l_3l_5c_5s_{23} \\
&\quad - s_{235}(p_{15} + p_{14}) - 2p_{20} \\
p_3 &= p_{11} + 2p_{13} - s_{235}(p_{14} + 3p_{16}) \\
&\quad + \frac{m_5l_5s_5}{2}(l_3c_{23} - l_2c_2) \\
p_4 &= p_{12} + p_{22} - p_{20} - s_{235}p_{15} + \frac{m_5l_3l_5c_5s_{23}}{2} \\
p_5 &= p_{12} + \frac{3}{2}p_{13} - s_{235}(p_{14} + p_{15} + 2p_{16}) - \frac{m_5l_3l_5s_5c_{23}}{2} \\
p_6 &= 2p_{13} - 2s_{235}p_{16} - \frac{m_5l_5^2s_5c_5}{2} \\
p_7 &= p_{21} + \frac{(m_5 + m_6)}{2}l_5^2s_{235}^2 + \frac{m_5l_5c_5}{2}(l_3c_{23} + l_2c_2) \\
&\quad + c_{235}p_{14} + I_5
\end{aligned}
$$

$$
\begin{aligned}
p_8 &= (m_5+m_6)\left(\frac{l_3l_5}{2}s_{23}s_{235}+\frac{l_5^2}{4}s_{235}^2\right)\\
&\quad +m\frac{m_5l_3l_5c_{23}c_5}{2}+c_{235}p_{15}+I_5\\
p_9 &= \frac{m_5l_5^2c_5^2}{4}+c_{235}p_{16}+I_5\\
p_{11} &= l_5c_{235}\left(\frac{m_5+m_6}{2}\right)\left(l_2s_2+l_3s_{23}+\frac{l_5}{2}s_{235}\right)\\
p_{12} &= l_5c_{235}\left(\frac{m_5+m_6}{2}\right)\left(l_3s_{23}+\frac{l_5}{2}s_{235}\right)\\
p_{13} &= \frac{l_5^2}{2}s_{235}c_{235}\left(\frac{m_5+m_6}{2}\right)\\
p_{14} &= m_6l_5\left(l_5c_{235}+l_3c_{23}+l_2c_2\right)\\
p_{15} &= m_6l_5\left(l_5c_{235}+l_3c_{23}\right)\\
p_{16} &= m_6l_5^2c_{235}\\
p_{17} &= l_5s_{235}\left(\frac{m_5+m_6}{2}\right)\left(l_2c_2+l_3c_{23}+\frac{l_5}{2}c_{235}\right)\\
p_{18} &= m_6l_5c_{235}\left(l_2s_2+l_3s_{23}+l_5s_{235}\right)\\
p_{19} &= \left(\frac{m_5+m_6}{2}\right)\left(2l_3c_{23}+l_5c_{235}\right)\\
p_{20} &= m_6l_5c_{235}\left(l_3s_{23}+l_5s_{235}\right)\\
p_{21} &= l_5s_{235}\left(\frac{m_5+m_6}{2}\right)\left(l_2s_2+l_3s_{23}\right)\\
p_{22} &= l_5s_{235}\left(\frac{m_5+m_6}{2}\right)\left(l_3c_{23}+\frac{l_5}{2}c_{235}\right)
\end{aligned}
$$

Taking the partial derivative of θ_5 in the Lagrange function yields

$$
\begin{aligned}
\frac{\partial L}{\partial\theta_5} &= n_1\dot\theta_2^2-p_{17}\dot\theta_1^2+n_2\dot\theta_3^2+n_3\dot\theta_5^2+n_4\dot\theta_2\dot\theta_3+n_5\dot\theta_2\dot\theta_5\\
&\quad +n_6\dot\theta_3\dot\theta_5-\frac{m_5}{2}gl_5c_{235}-m_6gl_5c_{235} \qquad (52)
\end{aligned}
$$

The coefficients of each item in the formula are expressed as

$$
\begin{aligned}
n_1 &= p_{11}+s_{235}p_{14}\\
n_2 &= p_{12}+s_{235}p_{15}\\
n_3 &= p_{13}+s_{235}p_{16}-\frac{m_5l_5^2c_5s_5}{2}\\
n_4 &= p_{11}+p_{12}+s_{235}\left(p_{14}+p_{15}\right)\\
n_5 &= p_{11}+p_{13}+s_{235}\left(p_{14}+p_{16}\right)-\frac{m_5l_5s_5}{2}\left(l_3c_{23}+l_2c_2\right)\\
n_6 &= p_{12}+p_{13}+s_{235}\left(p_{15}+p_{16}\right)-\frac{m_5l_3l_5s_5c_{23}}{2}
\end{aligned}
$$

According to (51) and (52), and considering the existence of disturbance d_5 in the system, the fifth dynamics equation can be obtained as

$$
\tau_5+d_5=\frac{d}{dt}\frac{\partial L}{\partial\dot\theta_5}-\frac{\partial L}{\partial\theta_5} \qquad (53)
$$

6) SOLUTION OF THE 6TH DYNAMICS EQUATIONS

Taking the partial derivative of $\dot\theta_6$ in the Lagrange function yields

$$
\frac{\partial L}{\partial\dot\theta_6}=I_6\left(\dot\theta_1+\dot\theta_4+\dot\theta_6\right) \qquad (54)
$$

Derivation of the above formula concerning time t can be obtained as

$$
\frac{d}{dt}\frac{\partial L}{\partial\dot\theta_6}=I_6\ddot\theta_1+I_6\ddot\theta_4+I_6\ddot\theta_6 \qquad (55)
$$

Taking the partial derivative of θ_6 in the Lagrange function yields

$$
\frac{\partial L}{\partial\theta_6}=0 \qquad (56)
$$

According to (55) and (56), and considering the existence of disturbance d_6 in the system, the sixth dynamics equation can be obtained as

$$
\tau_6+d_6=\frac{d}{dt}\frac{\partial L}{\partial\dot\theta_6}-\frac{\partial L}{\partial\theta_6} \qquad (57)
$$

In the text, $s_i=\sin(\theta_i)$, $s_{ij}=\sin\left(\theta_i+\theta_j\right)$, $c_i=\cos(\theta_i)$, $c_{ijk}=\cos\left(\theta_i+\theta_j+\theta_k\right)$.

D. SYSTEM MODEL DESCRIPTION

Based on the above solution of the P-Rob dynamics equations, we can see that the entire solution process is very complex. We obtain detailed expressions for each matrix in the system dynamics equation as shown in (58)–(60) at the bottom of the next page.

The parameters in the above three matrices are given by Section *C*. By looking up the coefficients obtained in Section *C*, we see that $q_8=j_7$, $q_9=p_7$, and $j_9=p_8$. This result confirms that the $M_0(\theta)$ matrix is a positive definite symmetric matrix, and the correctness of the solution to the dynamical model is further tested.

The solution provides a true understanding of the specific coupling relationships between the joint angles in the P-Rob robot manipulator system, which in turn facilitates the effective design of the control algorithm and the testing of the actual system dynamics model. The dynamics model can be described as follows

$$
\begin{cases}
M_0(\theta)\ddot\theta+C_0\left(\theta,\dot\theta\right)\dot\theta+G_0(\theta)=\tau+d\\
y=\theta
\end{cases} \qquad (61)
$$

In the above formula, $M_0(\theta)\in R^{6\times6}$ is the positive definite inertia matrix of the system, $C_0\left(\theta,\dot\theta\right)\in R^{6\times6}$ is the Coriolis force and centrifugal force, and $G_0(\theta)\in R^{6\times1}$ is the gravity term vector acting on the joint. All three matrices above are precise parts of the system model. d is the total of modeling error and external disturbance of the system, and τ is the control input to the system.

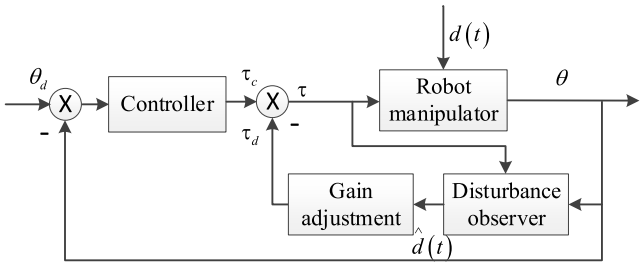

FIGURE 2. The frame structure of control system.

III. P-ROB SYSTEM CONTROL DESIGN

A block diagram of the control system is shown in Figure 2.

Figure 2 shows that θ_d is the desired predetermined trajectory of the system joints, θ is the actual trajectory of the system joints, the difference between θ_d and θ is used as the input of the controller, τ_c is the output control law of the integral sliding mode controller, τ_d is the control law of the output of the disturbance observer, τ is the actual input torque of the robot manipulator system, d is the total of modeling error and external disturbance of the system, and $\hat{d}$ is the estimated value of d.

A. DESIGN OF DISTURBANCE OBSERVER

To estimate the total disturbance of the system, in combination with (61), the nonlinear disturbance observer can be given by [37] and represented as follows

$$\dot{\hat{d}} = -L\hat{d} + L\left[M_0(\theta)\ddot{\theta} + C_0\left(\theta, \dot{\theta}\right)\dot{\theta} + G_0(\theta) - \tau\right] \tag{62}$$

Defining $\tilde{d} = d - \hat{d}$ as the disturbance tracking error, combined with (62) yields

$$\dot{\tilde{d}} = L\tilde{d} \tag{63}$$

The above equation can also be expressed as

$$\ddot{\tilde{d}} = \dot{d} - L\tilde{d} \tag{64}$$

In general, there is no a priori information about the derivative of the disturbance d. Designing it as $\dot{d} = 0$ means that the disturbance changes slowly concerning the dynamics of

$$M_0(\theta) = \begin{bmatrix} w_1 & 0 & 0 & I_4+I_6 & 0 & I_6 \\ 0 & q_7 & q_8 & 0 & q_9 & 0 \\ 0 & j_7 & j_8 & 0 & j_9 & 0 \\ I_4+I_6 & 0 & 0 & I_4+I_6 & 0 & I_6 \\ 0 & p_7 & p_8 & 0 & p_9 & 0 \\ I_6 & 0 & 0 & I_6 & 0 & I_6 \end{bmatrix} \tag{58}$$

$$C_0\left(\theta, \dot{\theta}\right) = \begin{bmatrix} -w_2\dot{\theta}_2 & 0 & -(w_{15}+w_{16})\dot{\theta}_3 & 0 & -w_{17}\dot{\theta}_1 & 0 \\ a_1\dot{\theta}_1 & (q_1-a_2)\dot{\theta}_2 + (q_4-a_5)\dot{\theta}_3 & (q_2-a_3)\dot{\theta}_3 + (q_6-a_7)\dot{\theta}_5 & 0 & (q_3-a_4)\dot{\theta}_5 + (q_5-a_6)\dot{\theta}_2 & 0 \\ -b_1\dot{\theta}_1 & (j_1-b_2)\dot{\theta}_2 + (j_4-b_5)\dot{\theta}_3 & (j_2-b_3)\dot{\theta}_3 + (j_6-b_7)\dot{\theta}_5 & 0 & (j_3-b_4)\dot{\theta}_5 + (j_5-b_6)\dot{\theta}_2 & 0 \\ 0 & 0 & 0 & 0 & 0 & 0 \\ (p_1+p_{17}) & -n_1\dot{\theta}_2 + (p_2-n_4)\dot{\theta}_3 & (p_4-n_2)\dot{\theta}_3 + (p_5-n_6)\dot{\theta}_5 & 0 & (p_6-n_3)\dot{\theta}_5 + (p_3-n_5)\dot{\theta}_2 & 0 \\ 0 & 0 & 0 & 0 & 0 & 0 \end{bmatrix} \tag{59}$$

$$G_0(\theta) = \begin{bmatrix} 0 \\ \left(\frac{m_2}{2}+m_3+m_4+m_5+m_6\right)l_2gc_2 + \left(\frac{m_3}{2}+m_4+m_5+m_6\right)l_3gc_{23} + \left(\frac{m_5}{2}+m_6\right)gl_5c_{235} \\ \left(\frac{m_3}{2}+m_4+m_5+m_6\right)l_3gc_{23} + \left(\frac{m_5}{2}+m_6\right)gl_5c_{235} \\ 0 \\ \left(\frac{m_5}{2}+m_6\right)gl_5c_{235} \\ 0 \end{bmatrix} \tag{60}$$

the disturbance observer. In this paper, it is assumed that the derivatives of the disturbance satisfy

$$\dot{d} = h(t) \tag{65}$$

where $h(t) \in L_2$ is the squared product, $d \in L_\infty$.

Further combining (64) yields

$$\dot{\tilde{d}} + L\tilde{d} = h(t) \tag{66}$$

When the gain matrix $L(\theta, \dot{\theta})$ is designed to be $L(\theta, \dot{\theta}) > 0$, it is asymptotically stable for all $\theta \in R^6$. Therefore, when $t \to \infty$, the estimation of disturbance $\hat{d}$ can approach d asymptotically, that is, $\lim_{t\to\infty} \hat{d} = \lim_{t\to\infty} d$, and the estimation error of disturbance can globally and asymptotically converge to zero. At the same time, the acceleration signal $\ddot{\theta}$ of the robot manipulator system cannot be measured to obtain effective information, so the selection of special $L(\theta, \dot{\theta})$ can also eliminate the acceleration nonlinear term contained in (62).

To obtain an estimate of the system disturbance d, the observer state auxiliary variable can be defined by [38] as

$$z = [z_1\ z_2\ z_3\ z_4\ z_5\ z_6]^T = \hat{d} - P(\theta, \dot{\theta}) \tag{67}$$

This is set here:

$$L(\theta, \dot{\theta}) M_0(\theta) \ddot{\theta} = \frac{dp(\theta, \dot{\theta})}{dt} \tag{68}$$

Combining (67) and (68) with (62) yields

$$\begin{aligned}\dot{z} &= \dot{\hat{d}} - L(\theta, \dot{\theta}) M_0(\theta) \ddot{\theta} \\ &= -L\hat{d} + L\left[M_0(\theta)\ddot{\theta} + C_0(\theta, \dot{\theta})\dot{\theta} + G_0(\theta) - \tau\right] \\ &\quad - L(\theta, \dot{\theta}) M_0(\theta) \ddot{\theta} \\ &= L(\theta, \dot{\theta})\left[C_0(\theta, \dot{\theta})\dot{\theta} + G_0(\theta) - \tau - z - P(\theta, \dot{\theta})\right]\end{aligned} \tag{69}$$

Here the relationship between the observed gain matrix $L(\theta, \dot{\theta})$ and the vector $P(\theta, \dot{\theta})$ satisfies

$$\begin{cases} L(\theta, \dot{\theta}) = XM^{-1}(\theta) \\ P(\theta, \dot{\theta}) = X\dot{\theta} \end{cases} \tag{70}$$

where X is a constant invertible matrix defined as

$$X = \begin{bmatrix} c_{11} & c_{12} & c_{13} & c_{14} & c_{15} & c_{16} \\ c_{21} & c_{22} & c_{23} & c_{24} & c_{25} & c_{26} \\ c_{31} & c_{32} & c_{33} & c_{34} & c_{35} & c_{36} \\ c_{41} & c_{42} & c_{43} & c_{44} & c_{45} & c_{46} \\ c_{51} & c_{52} & c_{53} & c_{54} & c_{55} & c_{56} \\ c_{61} & c_{62} & c_{63} & c_{64} & c_{65} & c_{66} \end{bmatrix}, \quad c_{ii} > 0, \quad i \in [1, 2, \ldots 6] \tag{71}$$

From (69), z is measurable and can only be determined by the angle and angle velocities without the acceleration signal. Combining (67), we obtain the approximation $\hat{d}$ for disturbance d.

$$\hat{d} = z + P(\theta, \dot{\theta}) \tag{72}$$

B. SYSTEM LINEARIZATION REPRESENTATION

Transforming (61), we get

$$\begin{aligned}\ddot{\theta} = M_0^{-1}(\theta)\tau + M_0^{-1}(\theta)\left(\hat{d} + \tilde{d}\right) \\ - M_0^{-1}(\theta)\left[C_0(\theta, \dot{\theta})\dot{\theta} + G_0(\theta)\right]\end{aligned} \tag{73}$$

Let: $\bar{\tau} = M_0^{-1}(\theta)\tau$, $\bar{d} = M_0^{-1}(\theta)\hat{d}$, $\nabla d = M_0^{-1}(\theta)\tilde{d}$, $f(\theta, \dot{\theta}) = -M_0^{-1}(\theta)\left[C_0(\theta, \dot{\theta})\dot{\theta} + G_0(\theta)\right]$.

Then, the above equation can be expressed as

$$\ddot{\theta} = \bar{\tau} + \bar{d} + f(\theta, \dot{\theta}) + \nabla d \tag{74}$$

Definition $\theta_i = \theta_{i1}$, $\theta_{i2} = \dot{\theta}_{i1}$, $i \in [1, \ldots, 6]$.

We rewrite the nonlinear dynamics equation represented by (74) in state-space form

$$\begin{cases} \dot{\theta}_{i1} = \theta_{i2} \\ \dot{\theta}_{i2} = \bar{\tau}_i + \bar{d}_i + f(\theta_i, \dot{\theta}_i) + \nabla d \\ y = \theta_i \end{cases} \tag{75}$$

where $f(\theta_i, \dot{\theta}_i)$ is the explicitly known quantity of the system, $\theta_i = [\theta_{i1}, \theta_{i2}]^T$ is the system state, y is the system output, $\bar{d}_i$ is the total disturbance estimate of the system, and $\bar{\tau}_i$ is the controlled object input.

We assume that the disturbance error ∇d of the system is bounded, i.e., $|\nabla d| \le D$. where $D \in R^+$, R^+ is the normal real number space.

At the same time, define the tracking error as $e = \theta_d - \theta_i$, $\dot{e} = \dot{\theta}_d - \dot{\theta}_i$, and $i \in [1, \ldots, 6]$.

The system control is designed so that the output of the system can effectively track the desired trajectory and keep the error close to zero, where θ_d is the desired motion trajectory of the system.

C. DESIGN OF NONLINEAR INTEGRAL SLIDING MODE SURFACE

The traditional integral sliding surface is

$$s = ce + \dot{e} + k\int_0^t e dt \tag{76}$$

where $c \in R^+$, and $k \in R^+$.

The traditional integral sliding mode surface cannot guarantee that the initial state is located on the switching surface, so the entire integral sliding mode surface inspired by [39] is designed as follows

$$s = ce + \dot{e} + k\int_0^t e dt - ce(0) - \dot{e}(0) \tag{77}$$

In the formula, $e(0)$ and $\dot{e}(0)$ respectively represent the initial values of θ_{i1} and θ_{i2} of the system state variables. It is easy to obtain $s(0) = 0$, which ensures that the initial moment of the system is located on the switching surface.

D. CONTROLLER DESIGN

The process of the sliding mode can be divided into two phases: the sliding phase of $s = 0$ and $\dot{s} = 0$ and the arrival phase of $s \neq 0$. Corresponding to these two different phases, the control is divided into two parts: equivalent control and switching control. Equation (77) is derived to obtain

$$\dot{s} = c\dot{e} + \ddot{e} + ke \tag{78}$$

When the above equation is equal to zero, the tracking error can be ensured to converge to zero asymptotically by selecting the appropriate gains $c > 0$ and $k > 0$ to achieve effective tracking of the trajectory.

Substituting the system model into the above formula, we have

$$\dot{s} = c\dot{e} + ke + \ddot{\theta}_d - \bar{\tau} - \bar{d} - f\left(\theta, \dot{\theta}\right) - \nabla d \tag{79}$$

When the system output is kept on the sliding mode surface, the total set disturbance of the system is zero, i.e., $\bar{d} + \nabla d = 0$. From $\dot{s} = 0$, we can obtain the equivalent control law as

$$\bar{\tau}_{eq} = c\dot{e} + ke + \ddot{\theta}_d - f\left(\theta, \dot{\theta}\right) \tag{80}$$

As external disturbances and parameter changes of the system can cause the initial output trajectory of the system to not lie on the sliding mode surface, the switching control law needs to be designed to drive the output trajectory of the system to the sliding mode. This process is called the arrival phase. For this purpose, we choose the Lyapunov function as

$$V = \frac{1}{2} s^T s \tag{81}$$

The selection of a suitable control strategy ensures that the error trajectory is switched from the arrival phase to the sliding phase and is also called the arrival condition. For

$$\dot{V} = s^T \dot{s} < 0, \quad s \neq 0 \tag{82}$$

to make the sliding mode reachability condition hold, the equivalent control law $\bar{\tau}_{eq}$ has been obtained thus far, and the control law $\bar{\tau}$ is now expanded by the switching control law $\bar{\tau}_{sw}$, which is

$$\bar{\tau} = \bar{\tau}_{eq} + \bar{\tau}_{sw} \tag{83}$$

We insert the system parameters and variables into the arrival condition (83) to obtain

$$\begin{aligned} \dot{V} &= s^T \dot{s} \\ &= s^T \left[c\dot{e} + ke + \ddot{\theta}_d - \left(\bar{\tau}_{eq} + \bar{\tau}_{sw}\right) - \bar{d} - f\left(\theta, \dot{\theta}\right) - \nabla d\right] \end{aligned} \tag{84}$$

Simple calculations, it follows that

$$\dot{V} = s^T \dot{s} = s^T \left(-\bar{\tau}_{sw} - \bar{d} - \nabla d\right) \tag{85}$$

Since the disturbance estimate $\bar{d}_i$ is a bounded known quantity, $\bar{\tau}_{sw}$ can be designed as

$$\bar{\tau}_{sw} = \zeta s + \mu sign\left(s\right) - \bar{d} \tag{86}$$

where μ is a positive real number indicating the upper limit of uncertainty. $\mu \in R^+$ $(\mu \geq D)$, $\zeta \in R^+$.

The derivative of Lyapunov time can be expressed as follows

$$\dot{V} = -\zeta s^T s - \mu \left|s\right| - s^T \nabla d \tag{87}$$

Lemma 1 ([40]): For any real numbers $\lambda_1 > 0, \lambda_2 > 0$, and $0 < \gamma < 1$, an extended Lyapunov condition of finite-time stability can be given as $\dot{V}(x) + \lambda_1 V(x) + \lambda_2 V^{\gamma}(x) \leq 0$, where the settling time can be estimated by $T_r \leq t_0 + \frac{1}{\lambda_1(1-\gamma)} \ln \frac{\lambda_1 V^{1-\gamma}(t_0) + \lambda_2}{\lambda_2}$.

The further derivation is as follows:

$$\begin{aligned} &s^T = [s_1 \cdots s_n]^T, \quad \Delta d = [\Delta d_1 \cdots \Delta d_n], \quad -s^T \Delta d \in R \\ &-s^T \Delta d = -\sum_{n=1}^{n} s_i \Delta d_i, \\ &\left|-s^T \Delta d\right| = \sum_{n=1}^{n} s_i \Delta d_i > 0, \\ &\left\|s^T\right\| = \left(\sum_{i=1}^{n} s_i^2\right)^{\frac{1}{2}}, \quad \|\Delta d\| = \left(\sum_{i=1}^{n} \Delta d_i^2\right)^{\frac{1}{2}}, \\ &\sum_{i=1}^{n} s_i \Delta d_i \leq \left(\sum_{i=1}^{n} s_i^2 \sum_{i=1}^{n} \Delta d_i^2\right)^{\frac{1}{2}} \\ &\left(\sum_{i=1}^{n} s_i^2 \sum_{i=1}^{n} \Delta d_i^2\right)^{\frac{1}{2}} = \left(\sum_{i=1}^{n} s_i^2\right)^{\frac{1}{2}} \left(\sum_{i=1}^{n} \Delta d_i^2\right)^{\frac{1}{2}} \\ &-s^T \nabla d \leq \left|-s^T \nabla d\right| \leq \left\|s^T\right\| \|\nabla d\| \leq D \left\|s^T\right\| \end{aligned} \tag{88}$$

$$\begin{aligned} \dot{V} &= -\zeta s^T s - \mu \left|s\right| - s^T \nabla d \\ &\leq -\zeta s^T s - \mu \left|s\right| - D \left\|s^T\right\| \\ &\leq -\zeta V - (\mu - D) V^{\frac{1}{2}} \end{aligned} \tag{89}$$

The system is finite-time asymptotically stable according to Lyapunov stability theorem. Therefore, the system control law can be designed as

$$\begin{aligned} \bar{\tau} = \bar{\tau}_{eq} + \bar{\tau}_{sw} = c\dot{e} + ke + \ddot{\theta}_d - f\left(\theta, \dot{\theta}\right) + \zeta s \\ + \mu sign\left(s\right) - \bar{d} \end{aligned} \tag{90}$$

IV. ANALYSIS OF SIMULATION RESULTS

The system dynamics equations established in this section and the validity of the controller design are further tested [41]. Using Simulink in MATLAB, the actual solved six-degree-of-freedom robot manipulator model obtained in this section is simulated and verified. And the control algorithm in the literature [42] is applied to this system, and then the comparison test of the two algorithms is realized. The inherent parameters of the system are as follow: $m_2 = 1$, $m_3 = 1$, $m_4 = 1.2$, $m_5 = 1$, $m_6 = 0.5$, $I_1 = 0.015$, $I_2 = 0.025$, $I_3 = 0.032$, $I_4 = 0.015$, $I_5 = 0.043$, $I_6 = 0.015$, $l_2 = 0.2$, $l_3 = 0.2$, and $l_5 = 0.2$. The system simulation parameters are set to initial angle $\theta_0 = [0.5\ 0.5\ 0.5\ 0.5\ 0.5\ 0.5]^T$, initial angle

velocity $\dot{\theta}_0 = [0\ 0\ 0\ 0\ 0\ 0]^T$, the total system disturbance is $d = 3 + \sin(t)/(1+t)$, $\mu = diag(10, 10, 10, 10, 10, 10)$, $c = diag(8, 8, 8, 8, 8, 8)$, $k = diag(5, 5, 5, 5, 5, 5)$, $\xi = diag(6, 6, 6, 6, 6, 6)$, acceleration of gravity $g = 9.8m/s^2$, and the expected trajectory of each joint is $\theta_d = \sin(\pi t)$. The control parameters are based on several simulated experiments and actual P-Rob platform experiments and finally selected in a trade-off between the best results of the two experiments.

Now the six-degree-of-freedom robot manipulator system is simulated using the control algorithm designed in this paper, and then the effectiveness of the algorithm design is verified. Since joints 1, 4, and 6 are parallel to each other and rotate in the same direction, and joints 2, 3, and 5 are parallel to each other and rotate in the same direction. Therefore, only the simulation results of trajectory tracking, velocity tracking, trajectory tracking error, control input and disturbance observation for joint 1 and joint 2 are displayed. The simulation results are shown as follows.

The control algorithm in the literature [42] is used for trajectory tracking and velocity tracking of the system, and the simulation results of joints 1 and 2 are presented.

Now consider applying constant disturbances as well as different time-varying disturbances in the system to further verify the effectiveness of the anti-disturbance integral sliding mode controller designed in this paper. These disturbances are designed as $d_1 = 3$, $d_2 = 3 + \sin t/(1+t)$, $d_3 = 3 + t/(1+t)$. Considering the space limitation, only the simulation results of joint 1 under different disturbances are represented as follows.

In the table, d is the different disturbances, e is the tracking error under different disturbances, which is obtained by making the deviation between the actual trajectory and the desired trajectory for each data point and finally adding and averaging them, and t is the time to reach stable tracking.

Using the control algorithm designed in this paper, the simulation results obtained are shown in Figure 3-figure 7. Figure 3 - figure 5 demonstrates the tracking effect of the system trajectory and velocity on the desired value, and the tracking error of the system position. We can see that the closed-loop system can reach a steady state in a short time. Figures 6 and 7 show the control input of the system and the state performance of the disturbance observer. It should be noted that the input signal of the closed-loop system is bounded and the disturbance observer effectively estimates the system disturbance in a short time, proving that the control algorithm designed in this paper has a good control performance. To further demonstrate the superiority of the control algorithm designed in this paper, we applied the control algorithm designed in the literature [42] to this research system and compared it with the simulation results in this paper for analysis. The simulation results of trajectory

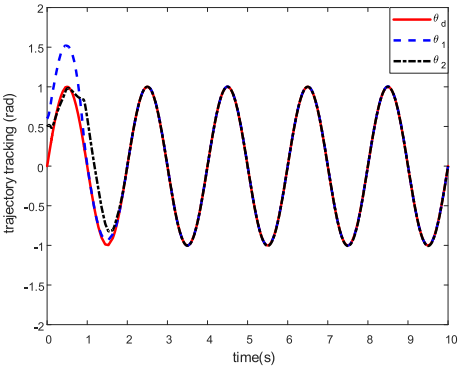

FIGURE 3. Joint 1, 2 trajectory tracking.

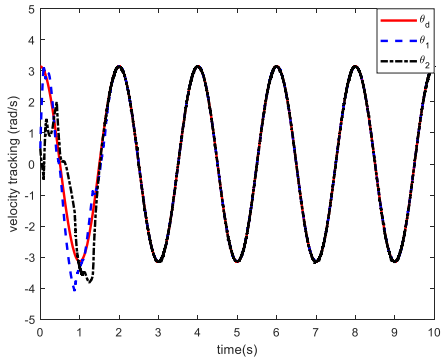

FIGURE 4. Joint 1, 2 velocity tracking.

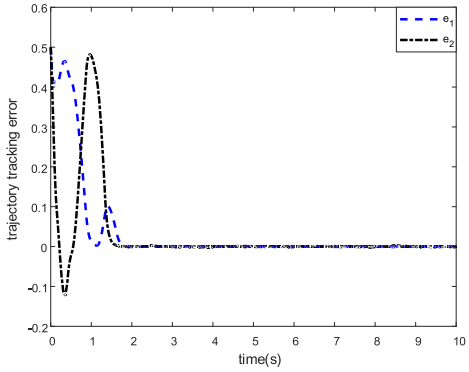

FIGURE 5. Joint 1, 2 trajectory tracking error.

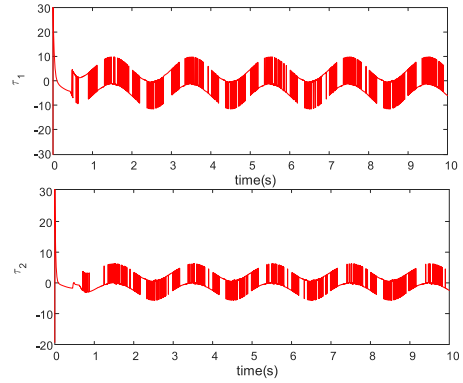

FIGURE 6. Joint 1, 2 control input.

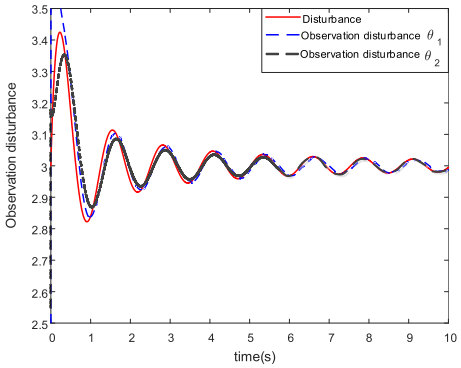

FIGURE 7. Joint 1, 2 observation disturbance.

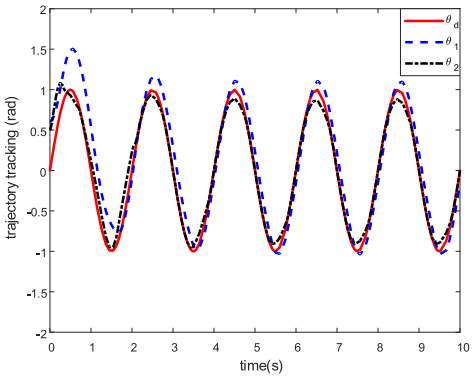

FIGURE 8. Joint 1, 2 trajectory tracking.

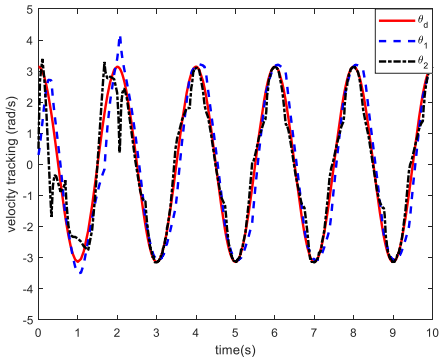

FIGURE 9. Joint 1, 2 velocity tracking.

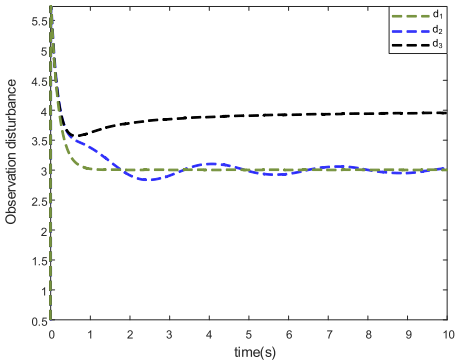

FIGURE 10. Observations under different disturbances.

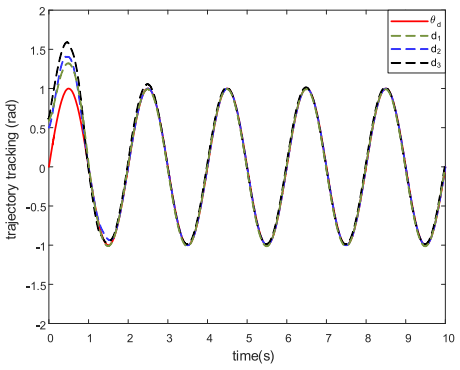

FIGURE 11. Joint 1 trajectory tracking under different disturbances.

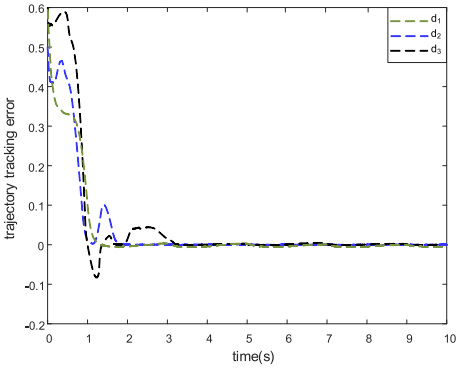

FIGURE 12. Tracking error of joint 1 trajectory under different disturbances.

tracking and velocity tracking for the control scheme proposed in the literature [42] are shown in figure 8 and figure 9, and we can see that the control scheme in the literature [42] is not very satisfactory for the control of the P-Rob system. The jitter vibration phenomenon is more obvious, and there is always an error in the trajectory tracking. To verify the robustness of the control algorithm designed in this paper, three different disturbances were selected to conduct numerical experiments on the system, and the experimental results are shown in Figures 10-12. Figure 10 shows the estimation effect of the system for different disturbances. Figure 11 depicts the trajectory tracking effect of the joint under the influence of different disturbances. Figure 12 depicts the tracking error of the trajectory of the joint under different disturbances. The analytical results of the experiments are shown in Table 1. The system can effectively estimate the constant disturbances or different time-varying disturbances, and achieve effective trajectory tracking in a short time, and the system can quickly reach the steady-state under the action of different types of disturbances, which indicates that the robustness of the control algorithm designed in this paper is good. The tracking control effect of the algorithm designed in this paper is more satisfactory, with smoother output, no abrupt changes, the jitter vibration phenomenon is suppressed, the tracking error converging to zero in a relatively short time, and the

TABLE 1. Tracking analysis under different disturbances.

d	e	t (s)
d_1	0.0484	1.21
d_2	0.0625	1.96
d_3	0.0750	3.13

robustness is strong. This system locates the initial state of the system on the sliding mode surface through the selection of the integral sliding mode surface, and the total disturbance is effectively compensated, so the simulation effect is better than the control algorithm in the literature [42]. Through simulation experiments of the two control algorithms, it can be seen that the dynamic performance index and static performance index of the control algorithm designed in this paper are better and achieve the design objectives. The entire control performance is satisfactory in terms of work effectiveness.

V. P-ROB PLATFORM EXPERIMENTAL ANALYSIS

In order to further investigate the practical value of the control algorithm designed in this paper, the designed control algorithm is now experimentally analyzed on the P-Rob platform. The P-Rob experimental platform has three wrist joints and three elbow joints, and it operates with a voltage limit of 100-240V AC, 50/60Hz, and maximum power consumption of 600W. The P-Rob is powered by a built-in 24V or 48V power supply with the battery embedded in its base. It has a total weight of 20 kg and a maximum payload of 3 kg at the end. The control of P-Rob is relatively simple and is web-based via myP software, with an intuitive web browser-based graphical user interface to control and communicate with P-Rob. The P-Rob experimental platform is shown in Figure 13.

FIGURE 13. Robot manipulator experimental platform.

Now, the P-Rob system is used to execute a series of experiments to grasp and put back a ping-pong ball. First, the path that the P-Rob system passes through in space is designed, and then the ideal motion trajectory of each joint of the P-Rob system is set according to the length of the P-Rob and the reachable range of the joints. The ideal motion trajectory of the end is formed by the motion of six joints. Finally, in the Application Editor window, the program for robot manipulator recognition is written in Python based on the designed anti-disturbance integral sliding mode control algorithm. The entire experiment is completed. The experimental results are shown in Figure 14.

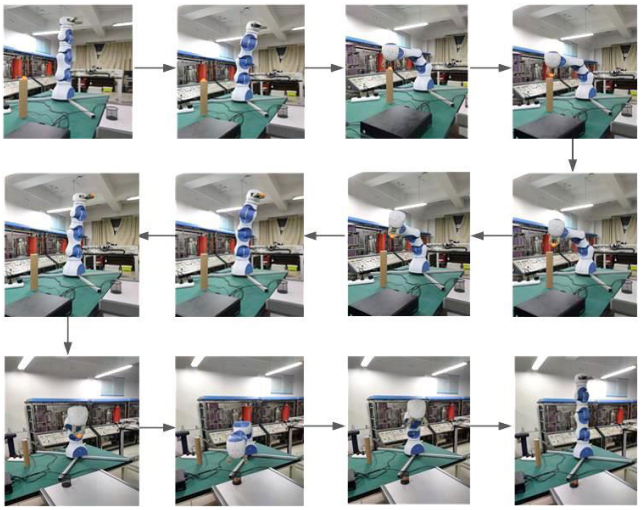

FIGURE 14. Process of grasping and placing movements of robot manipulator.

During the entire motion of the P-Rob system from the initial position to catching the ball, releasing it, and finally returning to the initial position, each joint moved according to the ideal trajectory that they each set, which realized the effective trajectory tracking of the P-Rob system. When an external disturbing torque is applied to the running robot manipulator, it is observed that under the action of the external torque, the robot manipulator first performs a jitter-removal pause and then puts it back into motion. This continuous process compared to the simulation results is the existence of a disturbance elimination time difference, this time difference can be understood as the system from the receipt of the external jitter signal, and then the controller issued to eliminate the disturbance command to reach the system actuator process. We perform 10 experiments, each experiment applied a different disturbance torque, and then the results of each experiment are compared with the simulation results of the same disturbance torque, the average value of the time difference is 1.273 seconds, this deviation robot manipulator system is very small in practical applications. Because this time difference is very short, the robot manipulator system quickly returns to a stable operating state. So the experimental results further confirm the effectiveness of the control scheme designed in this paper. Through experiments we observe that the entire process of catching ping-pong balls by the P-Rob system is fast and smooth, effectively tracking the desired trajectory and resisting external disturbances. This

fully reflects the rationality of the control algorithm design in this paper and that the theory can be combined with practice.

VI. CONCLUSION

In this paper, based on the Lagrange energy equation, a detailed solution of the lightweight P-Rob system is carried out to obtain the inertia, Coriolis force, and gravity matrices of the actual system model. The solution to the specific coupling equation for the P-Rob six-degree-of-freedom robot manipulator deepens the understanding of the robot manipulator system model. In a system simulation, a mathematical model solved for the actual P-Rob six-degree-of-freedom robot manipulator system is used. This is a simulation of great practical value.

To improve the trajectory tracking control accuracy under possible time-varying uncertain disturbances to the robot manipulator during operation, this paper combined the disturbance observer and integral sliding mode controller and proposed an integral sliding mode control algorithm based on the disturbance observer. The algorithm reduced the large adjustment gain of the control system, solved the shortcomings of the traditional sliding mode control system oscillation, improved the response speed, reduced the tracking error, the time-varying disturbances can be effectively suppressed, and enhanced the stability of the control system. A better tracking trajectory is obtained through simulation software, and experimental analysis is carried out on an actual six-degree-of-freedom P-Rob system. The practical value of the designed control algorithm is fully reflected by the experimental results, which provide a reference for the design of the mechanical mechanism of the robot manipulator and anti-disturbance control during motion in subsequent practical work.

REFERENCES

[1] L. R. Hochberg, D. Bacher, and B. Jarosiewicz, "Reach and grasp by people with tetraplegia using a neurally controlled robotic arm," *Nature*, vol. 485, no. 7398, pp. 372–375, May 2012.

[2] C. W. Coley, D. A. Thomas, J. A. M. Lummiss, J. N. Jaworski, C. P. Breen, V. Schultz, T. Hart, J. S. Fishman, L. Rogers, H. Gao, R. W. Hicklin, P. P. Plehiers, J. Byington, J. S. Piotti, W. H. Green, A. J. Hart, T. F. Jamison, and K. F. Jensen, "A robotic platform for flow synthesis of organic compounds informed by AI planning," *Science*, vol. 365, no. 6453, pp. 557–567, Aug. 2019.

[3] M. Agarwal, S. Biswas, C. Sarkar, S. Paul, and H. S. Paul, "Jampacker: An efficient and reliable robotic bin packing system for cuboid objects," *IEEE Robot. Autom. Lett.*, vol. 6, no. 2, pp. 319–326, Apr. 2021.

[4] A. M. Zanchettin, A. Casalino, L. Piroddi, and P. Rocco, "Prediction of human activity patterns for human–robot collaborative assembly tasks," *IEEE Trans. Ind. Informat.*, vol. 15, no. 7, pp. 3934–3942, Jul. 2019.

[5] H. Shen and Y.-J. Pan, "Tracking synchronization improvement of networked manipulators using novel adaptive nonsingular terminal sliding mode control," *IEEE Trans. Ind. Electron.*, vol. 68, no. 5, pp. 4279–4287, May 2021.

[6] J. Ni, L. Liu, Y. Tang, and C. Liu, "Predefined-time consensus tracking of second-order multiagent systems," *IEEE Trans. Syst., Man, Cybern. Syst.*, vol. 51, no. 4, pp. 2550–2560, Apr. 2021.

[7] D.-T. Tran, H.-V.-A. Truong, and K. K. Ahn, "Adaptive nonsingular fast terminal sliding mode control of robotic manipulator based neural network approach," *Int. J. Precis. Eng. Manuf.*, vol. 22, no. 3, pp. 417–429, Mar. 2021.

[8] V. Utkin, "Variable structure systems with sliding modes," *IEEE Trans. Autom. Control*, vol. 22, no. 2, pp. 212–222, Apr. 2003.

[9] D. B. Pham, J. Kim, S.-G. Lee, and K.-W. Gwak, "Double-loop control with hierarchical sliding mode and proportional integral loop for 2D ridable ballbot," *Int. J. Precis. Eng. Manuf.*, vol. 20, no. 9, pp. 1519–1532, Sep. 2019.

[10] M. Van, M. Mavrovouniotis, and S. S. Ge, "An adaptive backstepping nonsingular fast terminal sliding mode control for robust fault tolerant control of robot manipulators," *IEEE Trans. Syst., Man, Cybern. Syst.*, vol. 49, no. 7, pp. 1448–1458, Jul. 2019.

[11] H. Wang, Y. Pan, S. Li, and H. Yu, "Robust sliding mode control for robots driven by compliant actuators," *IEEE Trans. Control Syst. Technol.*, vol. 27, no. 3, pp. 1259–1266, May 2019.

[12] Z. Ma, Z. Liu, P. Huang, and Z. Kuang, "Adaptive fractional order sliding mode control for admittance-based telerobotic system with optimized order and force estimation," *IEEE Trans. Ind. Electron.*, early access, May 13, 2021, doi: 10.1109/TIE.2021.3078385.

[13] Z. Kuang, L. Sun, H. Gao, and M. Tomizuka, "Practical fractional-order variable-gain super-twisting control with application to wafer stages of photolithography systems," *IEEE/ASME Trans. Mechatronics*, early access, Feb. 19, 2021, doi: 10.1109/TMECH.2021.3060731.

[14] J. de Jesús Rubio, "Sliding mode control of robotic arms with deadzone," *IET Control Theory Appl.*, vol. 11, no. 8, pp. 1214–1221, May 2017.

[15] M. H. Rahman, M. Saad, J.-P. Kenné, and P. S. Archambault, "Control of an exoskeleton robot arm with sliding mode exponential reaching law," *Int. J. Control, Autom. Syst.*, vol. 11, no. 1, pp. 92–104, 2013.

[16] N. Kiem, N. Tinh, and B. Quyen, "Adaptive antisingularity terminal sliding mode control for a robotic arm with model uncertainties and external disturbances," *Turk. J. Electr. Eng. Comput. Sci*, vol. 26, no. 6, pp. 3224–3238, 2018.

[17] W. Yuan and G. Q. G. , "Disturbance observer-based adaptive integral sliding mode control for the hybrid automobile electro-coating conveying mechanism," *Int. J. Adv. Robot. Syst*, vol. 16, no. 3, pp. 1–12. May 2019.

[18] W.-H. Chen, "Disturbance observer based control for nonlinear systems," *IEEE/ASME Trans. Mechatronics*, vol. 9, no. 4, pp. 706–710, Dec. 2004.

[19] L. Han, G. Tang, R. Xu, H. Huang, and D. Xie, "Tracking control of an underwater manipulator using fractional integral sliding mode and disturbance observer," *Trans. Can. Soc. Mech. Eng.*, vol. 45, no. 1, pp. 135–146, Mar. 2021.

[20] M. Chen and W. H. Chen, "Sliding mode control for a class of uncertain nonlinear system based on disturbance observer," *Int. J. Adapt. Control Signal Process.*, vol. 24, no. 1, pp. 51–64, 2010.

[21] W.-H. Chen, D. J. Ballance, P. J. Gawthrop, and J. O'Reilly, "A nonlinear disturbance observer for robotic manipulators," *IEEE Trans. Ind. Electron.*, vol. 47, no. 4, pp. 932–938, Aug. 2000.

[22] K. Bai, X. Gong, S. Chen, Y. Wang, and Z. Liu, "Sliding mode nonlinear disturbance observer-based adaptive back-stepping control of a humanoid robotic dual manipulator," *Robotica*, vol. 36, no. 11, pp. 1728–1742, Nov. 2018.

[23] Z. Ma and P. Huang, "Adaptive neural-network controller for an uncertain rigid manipulator with input saturation and full-order state constraint," *IEEE Trans. Cybern.*, early access, Oct. 7, 2020, doi: 10.1109/TCYB.2020.3022084.

[24] M. Elsisi, K. Mahmoud, M. Lehtonen, and M. M. F. Darwish, "An improved neural network algorithm to efficiently track various trajectories of robot manipulator arms," *IEEE Access*, vol. 9, pp. 11911–11920, 2021.

[25] F. Caccavale, P. Chiacchio, and I. D. Walker, "A time-delayed observer for fault detection and isolation in industrial robots," *Robotica*, vol. 24, no. 5, pp. 557–565, Sep. 2006.

[26] J. Kim, "Two-time scale control of flexible joint robots with an improved slow model," *IEEE Trans. Ind. Electron.*, vol. 65, no. 4, pp. 3317–3325, Apr. 2018.

[27] H. Guo, Y. Liu, G. Liu, and H. Li, "Cascade control of a hydraulically driven 6-DOF parallel robot manipulator based on a sliding mode," *Control Eng. Pract.*, vol. 16, no. 9, pp. 1055–1068, 2008.

[28] A. Lopes and F. Almeida, "A force–impedance controlled industrial robot using an active robotic auxiliary device," *Robot. Comput.-Integr. Manuf.*, vol. 24, no. 3, pp. 299–309, Jun. 2008.

[29] G.-H. Xu, F. Qi, Q. Lai, and H. H.-C. Iu, "Fixed time synchronization control for bilateral teleoperation mobile manipulator with nonholonomic constraint and time delay," *IEEE Trans. Circuits Syst. II, Exp. Briefs*, vol. 67, no. 12, pp. 3452–3456, Dec. 2020.

[30] A. Jouila and K. Nouri, "An adaptive robust nonsingular fast terminal sliding mode controller based on wavelet neural network for a 2-DOF robotic arm," *J. Franklin Inst.*, vol. 357, no. 18, pp. 13259–13282, Dec. 2020.

[31] L. Kong, W. He, Y. Dong, L. Cheng, C. Yang, and Z. Li, "Asymmetric bounded neural control for an uncertain robot by state feedback and output feedback," *IEEE Trans. Syst., Man, Cybern. Syst.*, vol. 51, no. 3, pp. 1735–1746, Mar. 2021.
[32] M. Van and D. Ceglarek, "Robust fault tolerant control of robot manipulators with global fixed-time convergence," *J. Franklin Inst.*, vol. 358, no. 1, pp. 699–722, Jan. 2021.
[33] C. Veronneau, J. Denis, L.-P. Lebel, M. Denninger, V. Blanchard, A. Girard, and J.-S. Plante, "Multifunctional remotely actuated 3-DOF supernumerary robotic arm based on magnetorheological clutches and hydrostatic transmission lines," *IEEE Robot. Autom. Lett.*, vol. 5, no. 2, pp. 2546–2553, Apr. 2020.
[34] L. Zhou and S. Bai, "A new approach to design of a lightweight anthropomorphic arm for service applications," *J. Mech. Robot.*, vol. 7, no. 3, Aug. 2015, Art. no. 031001, doi: 10.1115/1.4028292.
[35] H. Yin, J. Liu, and F. Yang, "Hybrid structure design of lightweight robotic arms based on carbon fiber reinforced plastic and aluminum alloy," *IEEE Access*, vol. 7, pp. 64932–64945, 2019.
[36] A. Walsh and J. R. Forbes, "Modeling and control of flexible telescoping manipulators," *IEEE Trans. Robot.*, vol. 31, no. 4, pp. 936–947, Aug. 2015.
[37] S. P. Sadala and B. M. Patre, "Super-twisting control using higher order disturbance observer for control of SISO and MIMO coupled systems," *ISA Trans.*, vol. 106, pp. 303–317, Nov. 2020.
[38] J. Yang, S. H. Li, and X. H. Yu, "Sliding-mode control for systems with mismatched uncertainties vis a disturbance observer," *IEEE Trans. Ind. Electron*, vol. 63, no. 1, pp. 160–169, Jan. 2013.
[39] J. Shi, H. Liu, and N. Bajcinca, "Robust control of robotic manipulators based on integral sliding mode," *Int. J. Control*, vol. 81, no. 10, pp. 1537–1548, Oct. 2008.
[40] S. Yu, X. Yu, B. Shirinzadeh, and Z. Man, "Continuous finite-time control for robotic manipulators with terminal sliding mode," *Automatica*, vol. 41, no. 11, pp. 1957–1964, Nov. 2005.
[41] J. K. Liu, *MATLAB Simulation of Sliding Mode Variable Structure Control*. Beijing, China: Tsinghua Univ. Press, 2012.
[42] Z. Chen, Y. Zhang, Y. Zhang, Y. Nie, J. Tang, and S. Zhu, "Disturbance-observer-based sliding mode control design for nonlinear unmanned surface vessel with uncertainties," *IEEE Access*, vol. 7, pp. 148522–148530, 2019.

CHANG ZHANG received the B.S. degree in electrical engineering and automation and the M.S. degree in control science and engineering from Qufu Normal University, Qufu, China, in 2018 and 2021, respectively. He is currently pursuing the Ph.D. degree with Dalian Maritime University. His research interests include robot control and anti-disturbance control.

YUQIANG WU received the M.S. degree in automatic engineering from Qufu Normal University, Qufu, China, in 1988, and the Ph.D. degree in automatic control from Southeast University, Nanjing, China, in 1994. He is currently a Professor with the School of Engineering, Qufu Normal University, Rizhao, China. His current research interests include variable structure control, switching control, nonlinear system control, stochastic systems, and process control.